Stable isotopes as an effective tool for N nutrient source identification in a heavily urbanized and agriculturally intensive tropical lowland basin

Luu Thi Nguyet Minh[1], Do Thu Nga[2,5], Ioannis Matiatos[3], Virginia Natalie Panizzo[4], Trinh Anh Duc[5*]

[1] Institute of Chemistry, Vietnam Academy of Science and Technology, A18, 18 Hoang Quoc Viet, Cau Giay, Hanoi, Vietnam

[2] Electric Power University of Vietnam, 235 Hoang Quoc Viet, Cau Giay, Hanoi, Vietnam

[3] Isotope Hydrology Section, International Atomic Energy Agency, Vienna International Centre, PO Box 100, A-1400, Vienna, Austria

[4] School of Geography, Centre for Environmental Geochemistry, University of Nottingham, University Park, Nottingham, NG27 2RD, United Kingdom

[5] Nuclear Training Center, Vietnam Atomic Energy Institute, 140 Nguyen Tuan, Thanh Xuan, Hanoi, Vietnam

[*] trinhanhduc@vinatom.gov.vn or trinhanhduc@yahoo.com

Tel: +84906006808

Abstract

We present the application of dual stable isotope analyses of NO_3 (δ^{15}N-NO_3 and δ^{18}O-NO_3) to provide a comprehensive assessment of the provenance, partitioning, and conversion of nitrate across the Day River Basin (DRB), Vietnam, which is heavily impacted by agriculture and urbanization. Stable isotope compositions of river water δ^{18}O-H_2O, in addition to their δ^{15}N-NO_3 and δ^{18}O-NO_3 signatures, were

sampled at 12 locations in the DRB. Sample collection was conducted during three different periods to capture changes in regional weather and agricultural fertilization regimes; April (the dry season and key fertilization period), July (the rainy season and another key fertilization period) and October (the rainy season with no regional fertilization). Ranges of NO_3 stable isotopes are -7.1 to +9.2‰ and -3.9 to +13.2‰ for $\delta^{18}O$ and $\delta^{15}N$, respectively. Interpretation of the stable isotope data characterizes 4 main sources of NO_3 in the DRB; (1) nitrified urea fertilizer derived from an intensive agricultural irrigation network, (2) soil and groundwater leaching from within the basin (3) manure and sewage inputs (which is more prevalent in downstream river sections) and (4) upstream inflow from the Red River which discharges into the Day River through the Dao River. We applied a mixing model for the DRB consisting of 4 variables, representing these 4 different sources. The partition calculation shows that during the fertilization and rainy period of July, more than 45% of river NO_3 is derived from nitrified urea sources. During the other sampling periods (April and October), manure and sewage contribute more than 50% of river NO_3 and are derived from the middle portion of the DRB, where the Day River receives domestic wastewater from the Vietnamese capital, Hanoi. Stable isotope data of O and N reveal that nitrification processes are more prevalent in the rainy season than in dry season and that this predominantly takes place in paddy field agricultural zones. In general, data demonstrate that nitrate loss in the DRB is due to denitrification which takes place in polluted stretches of the river and dominates in the dry season. This study highlights that i) domestic waste should be treated prior to its discharge into the Day River and ii) the need for better catchment agricultural fertilization practices as large portions of fertilizer currently discharge into the river, which greatly impacts regional water quality.

Keywords: Vietnam, denitrification, nitrification, biological assimilation, dual stable isotopes

Introduction

The global nitrogen (N) cycle has been altered significantly since the mid C20th, in the advent of enhanced agricultural practices and accompanying fertiliser use (Galloway et al. 2004). Together with greater fossil fuel combustion and urbanisation (notably issues surrounding sanitation provision), agriculture has resulted in increased nitrogen fixation, which can ultimately impact upon other global biogeochemical cycles (including phosphorus and silicon) (Turner et al., 2003). Evidence for these impacts (most notably excessive fertilizer use and poor sewage treatment provision) upon the N cycle is documented via the N pollution of riverine environments around the world (Kendall 1998; Duc et al., 2007; Popescu et al., 2015; Vrzel et al., 2016). The consequences of increasingly higher N concentrations of rivers, is already exerting a strong influence on productivity and biodiversity of aquatic ecosystems (Galloway et al., 2004). As a consequence, more recent research has focused on understanding N fluxes in riverine catchments, the key transformation processes that are occurring (e.g. N. retention or denitrification) and thereby the impact that these have on downstream regions (Luu et al., 2012; Do et al., 2014). A comprehensive understanding of these transformation processes is the key to be able to fully budget N fluxes in these environments, which is particularly important in environments where distinct seasonality will exert a control upon biogeochemical processing (e.g. evidence of denitrification processes dominating in summer months; Panno et al., 2006). This is particularly relevant in tropical regions where strong monsoonal seasonality prevails. Such high rainfall intensities also enhance the potential for the high delivery of N fluxes to coastal regions (Do et al., 2019).

In order to address these issues, the application of nitrate N isotopes (δ^{15}N-NO_3), and more recently nitrate O isotopes (δ^{18}O-NO_3) provides an excellent means by which to trace the sources of N pollution in rivers. Furthermore, by applying these analyses in tandem permits an evaluation of the governing biogeochemical processes altering nitrate species in natural environments (Popescu et al., 2015; Vrzel et

al., 2016; Ta et al., 2016). The dual isotope approach is based on the principle that nitrate from different origins has distinct δ^{15}N-NO_3 and δ^{18}O-NO_3 isotopic signatures (see Kendall et al., 2007 for a review). For example, inorganic nitrate fertilizers have significantly higher δ^{18}O values (+17 to +25‰) compared to most other nitrate sources (e.g. soil, manure, sewage and inorganic NH_4 fertilizers are all not higher than +15‰), whereas their δ^{15}N composition is generally quite low (-5 to +6‰). In contrast, nitrate derived from organic sources tends to exhibit elevated δ^{15}N signatures (0 to +26‰), but comparatively low δ^{18}O values (-17 to +15‰) (Amberger & Schmidt 1987). For simple point-source analyses, these generalizations are useful. However, in anthropogenically impacted systems the situation may be more complex and there is a need to test this application fully. Here we provide one of the first applications of these analyses in a heavily anthropogenically impacted, tropical riverine system, the Day River Basin (DRB) in Vietnam. Here we assume that nitrate isotopic compositions of river waters will reflect both the regional and seasonal differences in nitrate source loading. Furthermore, they will also be modulated by in stream isotopic fractionation via processes such as denitrification, assimilation, and nitrification. The application of dual isotopic analyses of nitrate will allow us to assess isotopic fractionation associated with (1) nitrate removal processes (i.e., denitrification and assimilation), (2) nitrification, as well as to (3) identify inputs from multiple anthropogenic sources (Kendall et al., 2007; Burns et al., 2009; Widory et al., 2013; Michalski et al., 2015).

Indeed, several previous studies have indicated that in the Red River Delta (RRD) in northern Vietnam where the DRB is located, sewage and animal waste (which we also refer to as “anthropogenic organic” sources) inputs of N are greater than the amounts delivered from the river’s upstream watershed sources (Luu et al., 2012). Do et al. (2019) estimate that, annually, manure and sewage contribute more N to the river water than chemical fertilizers running off from regional paddy fields. However, the amounts of N ultimately delivered from the delta to the coastal zone are lower than the amounts carried by the river, showing extremely efficient nutrient retention in both soils and the drainage

network of the region (Seitzinger et al., 2006). Although relatively poorly constrained, denitrification and assimilation are considered to be the key nitrogen processes in the delta, with estimates of c. 59% of nitrogen being lost via these means (Quynh et al., 2005). Overall, these studies have used the approaches of subtracting nutrient inputs from the DRB and its output at the river mouth (Quynh et al., 2005; Luu et al., 2012; Do et al., 2014), which cannot estimate i) the relative proportion of differing NO_3 sources discharging to the river and ii) the in-stream processes taking place. In this study, we aim to improve these estimates via the use of stable isotope and mass balance approaches. The nitrate isotopes are used here as the key variables to (1) quantify dominant sources of nitrate and (2) to assess the key biogeochemical processes that control the in stream production and reduction of nitrate in the DRB, a highly populous, urbanized landscape set in a tropical, lowland delta region.

Materials and methods

Study site description

Vietnam is the second largest rice exporter in Asia, with it's cultivation area having increased from 4.7 Mha in 1961 to 7.3 Mha in 2007. Concurrently, the application of nitrogen fertilizers in Vietnam has increased 7.2% annually since 1985. Such intensive use of chemical fertilizers has been recognized as a potential source of environmental pollution in the region (Luu et al., 2012: Do et al., 2019). This is particularly notable in the DRB (Fig. 1), where rice cultivation constitutes approximately 50% of land use and the majority of the fertilizer used is applied to paddy fields (DARD-Hanoi 2009; DARD-Namdinh 2011; Kurosawa et al. 2004; Kurosawa et al. 2006). These chemical fertilizers applied within the DRB are the primary sources of N in the Day River (MONRE 2006; Hanh et al. 2010). Along with the expansion of rice agriculture, the country's production of livestock has also increased 3 times since its economic

reform in the 1980s (GSO 2014). On top of that, urbanization in the DRB is rapid, associated with development in and around Hanoi, the capital of Vietnam, is located here.

<Fig. 1 close to here>

The DRB covers 7,665 km^2 and includes all of Ha Nam, Nam Dinh, and Ninh Binh Provinces, as well as a part of Hanoi and Hoa Binh Provinces (MONRE 2006). The total population of the area is approximately 11.7 million (GSO 2016). At present, this river system is under considerable pressure from socioeconomic development activities and urbanization, and the basin is experiencing an annual population increase of about 5% (MONRE 2006). However, the region's infrastructure (irrigation, drainage, traffic systems, urban planning, waste collection and treatment) is not being developed at an equivalent rate and so is unable to accommodate such rapid growth (Do & Nishida 2014). The establishment and operation of industrial zones, including craft villages, factories and agricultural areas, has caused significant changes to the natural environment, especially regional water quality (Duc et al., 2007). Given the existing level of infrastructure and the provision of its resources, most solid and liquid waste is not being treated but rather discharged directly to the surrounding water bodies and waterways. Do & Nishida (2014) reported more than 156,000 industrial, commercial and service establishments discharge about 100,000m^3 of wastewater per day to the river. They also tallied about 133 hospitals in DRB, which discharge a total of 27,686 m^3 of hospital wastewater per day to the drainage system without treatment. Rather, only 3.61% of wastewater in the river basin has been treated by wastewater treatment plants (Do & Nishida 2014). Water regimes in the upstream part of Day River are largely controlled by a system of sluice gates and pumping stations, to allocate water for different purposes (e.g. irrigation and draining or preventing urbanized areas from seasonal inundation). Agriculture is also an important activity in this basin. Rice paddies occupy 2,414 km^2 with two rice seasons; spring fields are cultivated from late January to late May, and summer fields are cultivated

from early June to late September. Application rates of chemical fertilizer for spring and summer growing seasons are 13,340-16,100 and 7,660-8,900 kg N km^{-2}, respectively (MARD 2008).

Sampling and analyses

In order to identify the sources and assess the processes controlling NO_3 in the DRB, water sampling was conducted at 12 locations upstream and downstream of the Day River's confluences with its tributaries (Fig. 1). The main stream of Day River receives water from 5 main tributaries; named in order from upstream, Bui River, Nhue River, Hoang Long River, Sat River, and Dao River. Among those tributaries, Bui and Hoang Long Rivers bring water from fairly pristine-mountainous catchments characterized by degraded forests growing on a limestone landscape. The Nhue River is well-known for discharging domestic wastewater from the Hanoi Metropolis (Trinh et al. 2012). The Sat River flows through areas of land irrigated and drained for agricultural purposes in the DRB. The Dao River is a man-made canal connecting the Day and Red Rivers. This man-made canal helps divert a large volume of water from the Red River to the Day River (Luu et al. 2010).

Table 1: Names and locations of the sampling stations, refer to Fig. 1 for their special location

Station name	River reach	Longitude (°E)	Latitude (°N)	Altitude (m)	Distance to the next downstream point
Phung (D1)	Upstream	105.64513	21.07521	12	30 km to D2
Mai Linh (D2)	Upstream Bui River's confluence	105.72711	20.93646	11	30 km to D3
Ba Tha (D3)	Confluence with Bui River	105.70722	20.80583	10	25 km to D4
Te Tieu (D4)	Downstream Bui River's confluence	105.74710	20.68646	9	35 km to D5

Que (D5)	Upstream Nhue River's confluence	105.87263	20.57451	8	9 km to D6
Ba Da (N2)	Nhue River mouth	105.92192	20.56717	8	6 km to D6
Do (D6)	Downstream Nhue River's confluence	105.91151	20.51578	7	20 km to D7
Doan Vi (D7)	Upstream Hoang Long River's confluence	105.92081	20.36240	3	20 km to D8
Non Nuoc (D8)	Downstream Hoang Long River's confluence and upstream Sat River's confluence	105.98071	20.26526	3	15 km to D9
Do Thong (D9)	Downstream Sat River's confluence and Upstream Dao River's confluence	106.04511	20.21738	2	25 km to D10
Do Muoi (D10)	Downstream Dao River's confluence (Day River receives the Red River water through Dao River)	106.16600	20.14200	1	20 km to D11
Cua Day (D11)	Day River mouth, estuarine zone	106.10300	19.92800	0	3 km to the Sea

146

147 Due to the seasonality of the region (namely a tropical monsoon climate), we selected 3 periods of
148 sampling to capture the variability in regional weather regimes (namely the wet and dry seasons). This is

149 also mirrored in terms of the agricultural fertilization application regimes for the area. This sampling
150 approach permitted a full assessment of nitrate sources to the DRB as well as key transformation
151 processes at different periods of the year. Sampling was conducted in October 2016 (the rainy season
152 and regional non-fertilization period), July 2017 (the rainy season and regional fertilization period), and
153 April 2018 (the dry season and regional fertilization period). Sampling was not conducted at stations D1-
154 D5 in the July 2017 sampling campaign.

155 River waters were sampled at a distance of approx. 10 m from river banks and divided into sub-samples
156 for analysis of N nutrient concentrations, Dissolved Organic Carbon (DOC), and stable isotope analyses.
157 These parameters were chosen as it is acknowledged that to assess the sources of NO_3 and to identify
158 the governing processes of NO_3 in stream water, stable isotopes of water ($\delta^{18}O$-H_2O), N species and
159 carbon availability (represented as DOC) should also be analysed (Baker and Vervier, 2004; Zarnetske et
160 al., 2011; Ta et al., 2016).

161 For water stable isotope analyses, sub-samples were filtered in the field with Sartorius technical filter
162 papers (8 μm pore size) and collected in 30 ml HDPE plastic bottles. They were then kept at 20°C prior to
163 be sent to the Isotope Hydrology Laboratory of the International Atomic Energy Agency (IAEA), Vienna,
164 Austria for analysis. All samples were pipetted into 2 mL laser vials, and high-precision measured using a
165 Los Gatos Research liquid water isotope analyzer model 912-0032 (Los Gatos Research (www.lgrinc.com,
166 California, USA)). The method consisted of 9 injections per vial and ignoring the first 4, with data
167 processing procedures to correct for between-sample memory and instrumental drift, and normalization
168 to the VSMOW-SLAP scale using LIMS for Lasers 2015 as fully described elsewhere (Wassenaar et al.
169 2014; Coplen & Wassenaar 2015). A 2-point normalization was used using IAEA laboratory standards W-
170 34 (low standard) and W-39 (high standard) to bracket the isotopic composition of the samples. IAEA
171 laboratory standards were calibrated using VSMOW2 and SLAP2 primary reference materials using their

assigned of values of 0±0.3‰, 0±0.02‰, and -427.5±0.3‰, -55.5±0.02‰ for δ^2H and $\delta^{18}O$, respectively. The assigned values for the laboratory calibration standards W-39, W-34 and control W-31 were +25.4±0.8‰ and +3.634±0.04‰; -189.5±0.9‰ and -24.778±0.02‰; -61.04±0.6‰ and -8.6±0.09‰ for δ^2H and $\delta^{18}O$ relative to VSMOW, respectively. The control W-31 long-term (1-yr running average) analytical reproducibility (±SD) was ±0.11‰ and ±0.7‰ for $\delta^{18}O$ and δ^2H, respectively.

The sub-samples for dual stable isotope analysis of NO_3 were filtered with GF/F Whatman filters, stored in acid-cleaned, high-density polyethylene (HDPE) bottles and frozen prior to be sent also to the Isotope Hydrology Laboratory of IAEA for analysis. The Cd-azide reduction method to headspace N_2O gas was used as fully described in McIlvin & Altabet (2005). The instrument used was an Isoprime 100 with a Trace Gas (TG) system linked to a continuous flow isotope ratio mass spectrometer (CF-IRMS) system (Isoprime Ltd, Cheadle Hulme, UK). The Isoprime CF-IRMS system operated at an external analytical precision of ±0.2‰ ($\delta^{15}N$-N_2O values) and ±0.3‰ ($\delta^{18}O$-N_2O values) using 2-point normalization using dissolved nitrate reference materials (USGS32, USGS34, USGS35, IAEA NO3).

The analytical procedures for dissolved nitrogen compounds were conducted in the Institute of Chemistry (ICH), Vietnam Academy of Science and Technology (VAST), in accordance with the Standard Methods for the Examination of Water and Wastewater (Clesceri et al. 1998). The 1 L sub-samples were kept below 4^{o}C to prevent significant degradation during storage, and analyzed within 48 hours. Nitrate was determined by quantitative reduction to nitrite on a cadmium column, followed by colorimetric determination at 540 nm of nitrite using the Griess reaction (Standard method 4500-NO_3 E in Clesceri et al. (1998). Detection limit (DL) of the NO_3 analysis was 0.02 mg NO_3 L^{-1}. Analytical protocols of nitrite (NO_2) was similar to NO_3 but without the reduction step. The DL of this method was 0.005 mg N L^{-1}. Ammonium (NH_4) was determined colorimetrically at 640 nm by the phenol hypochlorite method (Standard method 4500-NH3 F. phenate in Clesceri et al. 1998). The Kjeldahl digestion method was used

for total nitrogen (N_{tot}) analysis as described in the Total Kjeldahl Nitrogen (TKN) method (Standard method 4500-Norg B) of Clesceri et al. (1998). The spectrometer used for colorimetric determination was an UV-VIS GBC Cintra 40 (Australia). Organic nitrogen (N_{org}) was simply subtracted from N_{tot} minus inorganic N species (NO_3, NO_2, and NH_4).

Sub-samples for DOC analysis were filtered on Whatman GF/F glass filters (filters were heated at 550°C in a furnace for 4 hours to remove organic matter contaminant) and stored in the 10 ml glass tubes prior to be analyzed in VAST. Each sample tube was doped with 10 µl of concentrated (98%) analytical grade H_3PO_4 and kept in refrigerator prior to analysis. Analysis of DOC was performed on a TOC-Ve (Shimadzu, Japan) with a triplicate reading mode.

Mixing model formulation

We considered the following four main sources of nitrate based on the geographical and natural conditions of the DRB (e.g. Thibodeau et al. 2013; Ta et al. 2016): (1) inputs from soil and groundwater sources (representing natural, background input levels), (2) inputs from the Red River (also considered as natural sources), (3) inputs from regional, excessive application rates of chemical fertilizers (urea), and (4) inputs from organic matter deriving from urban regions and livestock farming (sewage and manure). In order to derive the proportion that these sources derive in the DRB, we used the following partition equations of NO_3, which are based on our stable isotope data:

$$\delta^{18}O = f_S\delta^{18}O_S + f_P\delta^{18}O_P + f_U\delta^{18}O_U + f_M\delta^{18}O_M \quad (1)$$

$$\delta^{15}N = f_S\delta^{15}N_S + f_P\delta^{15}N_P + f_U\delta^{15}N_U + f_M\delta^{15}N_M \quad (2)$$

$$1 = f_S + f_P + f_M + f_U \quad (3)$$

Of which f_S, f_U f_P, and f_M are respectively the partition coefficients of each of the 4 main sources (as listed above): 1) soil and groundwater input (f_S), 2) Red River inflow (f_U), 3) nitrified urea fertilizer run-off from paddy fields (f_P) and 4) sewage and manure discharge (f_M).

Since the mixing model has three equations (Eq. 1, 2, and 3) and four variables (f_S, f_P, f_U, and f_M) which mathematically cannot be solved, we had to make further assumptions to deduce a variable (or add an equation). In the DRB, the Red River fraction (f_U) only exists at D10 and D11 (Fig. 1) where the Dao River discharges water into the Day River (Trinh et al. 2017). Thus, from D1 to D9, there are essentially only three variables (f_S, f_P, and f_M) which permit the three equations to be solved. Therefore at sites D10 and D11, we used additional information of water stable isotopes and nitrate concentrations to estimate the variable f_U (Eq. 4, 5, and 6) so as to calculate the three other variables (f_S, f_P, and f_M) and apply our mixing model.

$$\delta^{18}O\text{-}H_2O_{D10} = f_{D9}\delta^{18}O\text{-}H_2O_{D9} + f_{Dao}\delta^{18}O\text{-}H_2O_{Dao} \quad (4)$$

$$C_{NO_3,D10} = f_{D9}C_{NO_3,D9} + f_{Dao}C_{NO_3,Dao} \quad (5)$$

$$1 = f_{D9} + f_{Dao} \quad (6)$$

Where f_{D9} and f_{Dao} are respectively flow/discharge fractions of D9 and Dao River (Red River input) at D10. C_{NO3} represents the concentration of NO_3 at different points. In fact, $f_{Dao}*C_{NO3,Dao}$ and $f_{D9}*C_{NO3,D9}$ are respectively corresponding to $f_{u,D10}$ and $f_{S,D10} + f_{p,D10} + f_{M,D10}$. In other words:

$$\frac{f_{Dao}C_{NO_3,Dao}}{f_{U,D10}} = \frac{f_{D9}C_{NO_3,D9}}{f_{U,D10}+f_{P,10}+f_{Ur,D10}} \quad (7)$$

As $\delta^{18}O\text{-}H_2O$ in the Dao River is provided here, this equation was used to estimate the Red River input partition coefficient (f_U) at D10 and D11.

235 Of these 4 different sources applied in our mixing model (our end members), the soil and groundwater
236 (*fs*) and the chemical fertilizer (*fp*) concentrations and compositions were derived from other studies
237 taken in the RRD. For the soil and groundwater (otherwise naturally released) sources, a comprehensive
238 isotopic analysis of dissolved N species in soil and groundwater for the Hanoi region was reported in
239 Giap et al. (2007). Oxygen isotope ($\delta^{18}O\text{-}NO_3$) signatures were extracted from the work of Saiki et al.
240 (2019) who carried out a comprehensive study of nitrate isotopes within a sub-basin of the RRD, which
241 neighbors the DRB. Nitrogen isotopes of nitrate excess from the application of urea fertilizer in paddy
242 fields were also taken from the study of Saiki et al. (2019), which was in the range of fertilizer nitrogen
243 isotope signatures reviewed in Bateman & Kelly (2007). Oxygen isotope ($\delta^{18}O\text{-}NO_3$) end members were
244 further calculated from the analyzed water stable oxygen isotope ($\delta^{18}O\text{-}H_2O$) and atmospheric oxygen
245 isotope (+23.5‰) based on recent studies about isotope fractionation during nitrification (Casciotti et
246 al., 2010; Buchwald & Casciotti, 2010). Detailed formulation of this calculation is shown in the appendix.
247 Analytical results of samples taken at N2 in the Nhue River were used as the manure and sewage source
248 based on the fact that the Nhue River is the main open-air sewer of the Hanoi metropolis (Duc et al.,
249 2007). For the Red River inflow, the additional analysis of 2 samples taken at sites in the Red River (sites
250 of Ha Noi and Nam Dinh as represented in Trinh et al., 2017) provided data and these were used as the
251 Red River inflow end member. All end member isotopic compositions are shown in Table 2.

252

253 Table 2: End member compositions of $\delta^{18}O$ and $\delta^{15}N$ of nitrate used in this study for the partition calculations. Values for each of the three

254 sampling periods (and seasons) are displayed with their respective standard deviations.

	Literature review				This study			
	Soil and ground (natural leaching)		Paddy fields (nitrified urea fertilizer run-off)		Red River (natural inflow)		Manure and sewage (anthropogenic organic N)	
	$\delta^{18}O$ [(a)]	$\delta^{15}N$ [(b)]	$\delta^{18}O$ [(c,d)]	$\delta^{15}N$ [(a,e)]	$\delta^{18}O$ [(c)]	$\delta^{15}N$ [(c)]	$\delta^{18}O$ [(c)]	$\delta^{15}N$ [(c)]
Dry, fertilizing	7.8±0.3 (2)	4.5±1.0 (40)	-7.6±2.9 (32)	-5.9±0.3 (2)	6.3±1.8 (2)	6.5±1.2 (2)	0.59 (1)	16.2 (1)
Rainy, fertilizing	5.0±0.3 (3)	4.5±1.0 (40)	-9.1±3.1 (32)	-5.9±0.3 (2)	1.8±0.7 (2)	7.9±0.1 (2)	-1.26 (1)	16.2 (1)
Rainy, non-fertilizing	2.5±0.3 (2)	4.5±1.0 (40)	-10.4±3.0 (32)	-5.9±0.3 (2)	1.1±1.1 (2)	5.2±0.4 (2)	-2.87 (1)	16.2 (1)

255 Numbers in ( ) indicate sample size

256 [(a)] Saiki et al. (2019)

257 [(b)] Giap et al. (2007)

258 [(c)] Our analytical results

259 [(d)] Casciotti et al., 2010 and Buchwald & Casciotti, 2010

260 [(e)] Bateman and Kelly (2007)

It should be noted that we acknowledge the uncertainties surrounding source values due to the limited availability of data (on NO_3 isotopes) for this region. In particular, the mean and standard deviations calculated from our small data set do not permit a normal distribution check and so we may only partly represent the true variability of the NO_3 sources in the DRB. However, we highlight the importance of these attempts in elucidating pollution sources and N cycle processing taking place in this highly disturbed catchment of northern Vietnam. In addition, there other are sources of uncertainty which are beyond our control (e.g. the analytical uncertainties of data from cited literature, and limitations surrounding their differing geographical locations, seasonality and/or time periods).

The Monte Carlo simulation run on the platform of Excel Visual Basic Macro was employed to analyze the uncertainty of the partition computation. As introduced in Do et al. (2014), we first decided the distribution type and specified the standard deviation values for each end member isotope composition based on our literature review (Giap et al., 2007; Bateman & Kelly 2007; Casciotti et al., 2010; Buchwald & Casciotti, 2010; Saiki et al., 2019) and our analytical results. Next we reformulated our mixing model equations to embed it into the Excel platform. Then, we ran the Monte Carlo simulation and obtained 1,000 values for nitrate source components and get the uncertainty ranges of target parameters (source component fractions).

Statistical analyses

Correlation coefficient calculation was used to assess the correlations between i) isotopic variables and ii) the isotopic variables and other variables. Principal component analysis (PCA) was used to define the principal processes governing the variability of analytical results (including the isotopes, all N species, and DOC) over the upstream sites (D1-D5). The PCA was run separately for April and October data in order to assess the seasonality of biogeochemical processing. Note, we did not run the PCA analysis for

283 the downstream sites for comparison as NH_4 and NO_2 were, for the most part, below the analytical
284 detection limit. All statistical tests were performed using the statistical Origin software, version 2019b.

285 # Results

286 ## Seasonal and spatial distribution of DOC, nitrogen species, and NO_3 stable isotope
287 ## signatures

288 <Fig. 2 close to here>

289 The dominant N species was NO_3 (accounting for >50% of total N, especially in the middle section of the
290 river; Fig. 2a-d). In general, nitrate was higher in the middle section than in the upstream and
291 downstream sections of the Day River, with the highest concentration (4.1 mg-N L^{-1}) at site D6 in the
292 April survey (the dry season) (Fig. 2a). The lowest nitrate concentrations were also found in April at the
293 upstream site of D2 (0.1 mg-N L^{-1}). Nitrite was the least concentrated among N species (Fig. 2b). In
294 general, NO_2 was lower than 0.3 mg-N L^{-1} and spatially there was no clear downstream trend for the Day
295 River. Ammonium was generally lower than detection limit (0.015 mg-N L^{-1}) in downstream sites (D9-
296 D11) (Fig. 2c). Like NO_3, total nitrogen was higher in the dry (April) rather than in the rainy season (Fig.
297 2a, d) while NH_4 was lower in the dry season (rather than in the rainy season months of July and
298 October) (Fig. 2c). Organic nitrogen, like NO_3 and N_{tot}, was higher in middle section than in upstream and
299 downstream sections. DOC concentrations were generally higher in April compared to July and October
300 sampling periods (fig. 2e). The correlation between DOC and Organic nitrogen was positively weak. The
301 correlation coefficients in April, July, and October were 0.10 (p_value = 0.78), 0.17 (p_value = 0.62), and
302 0.07 (p_value = 0.85), respectively, while the DOC/Organic nitrogen ratio averaged at 12.5.

303 Water oxygen isotope signatures ($\delta^{18}O$-H_2O) did not change much between sites D1 to D9 but decreased
304 sharply (nearly 2‰) after site D9, during the rainy season (Fig. 2f). While during the dry season, water
305 oxygen isotope compositions were low in upstream (-5.78‰ at D2) and downstream (-8.6‰ at D10)
306 reaches of the DRB, they remained high in the middle sections (-2.63‰ at D5). Average values of $\delta^{18}O$-
307 H_2O in April, July, and October were -4, -6.2, and-8‰ respectively.

308 <Fig. 3: close to here >

309 In general, the oxygen isotope composition of nitrate ($\delta^{18}O$-NO_3) varied between -7.1 and +9.2‰ (Fig.
310 3a).This range of $\delta^{18}O$-NO_3 was lower than the range usually found in inorganic fertilizer NO_3 (>+20‰,
311 (Amberger & Schmidt 1987)) and atmospheric deposition of NOx (>+30‰, (Kendall et al. 2007)) sources,
312 corresponding well with urea being the main N fertilizer utilized in this deltaic region. Seasonally, $\delta^{18}O$-
313 H_2O and $\delta^{18}O$-NO_3 data displayed similar trends, as signatures for both were highest in April, followed by
314 July, and then October (fig. 2f and 3a).

315 Overall, the range of $\delta^{15}N$-NO_3 fell between -3.9 to +13.2‰ which covers most sources of $\delta^{15}N$ usually
316 found in surface waters (N sources from chemical fertilizers to soil, manure and sewage) (Fig. 3b).
317 Spatially, the variation observed for $\delta^{15}N$-NO_3 on the upper reaches of watersheds was higher than that
318 observed further downstream (after D8). Seasonal changes in $\delta^{15}N$-NO_3 were greater in upstream
319 reaches compared to the downstream sites (Fig. 3b).

320 Correlation coefficient between the nitrate isotopes for the whole dataset was 0.39 (p_value = 0.05). For
321 each of the three field campaigns, variations in $\delta^{18}O$-NO_3 and $\delta^{15}N$-NO_3 data were not well correlated
322 (Fig. 4). Correlation coefficients between the 2 variables in April, July, and October were -0.21 (p_value =
323 0.56), 0.41 (p_value = 0.40), and 0.15 (p_value = 0.68), respectively. The correlation coefficient between
324 $\delta^{18}O$-NO_3 and ln(NO_3) was -0.73 (p_value = 0.01) in October (wet season). In April, the correlation

325 coefficient was lower (= -0.47, p_value = 0.17). In addition, correlation coefficients of upstream sites
326 (D1-D5) are shown in table 3. In both periods, correlation coefficients between $\delta^{18}O\text{-}NO_3$ and NO_3 were
327 negative. Isotopic signatures appeared to be more correlated with each other and with DOC in April,
328 than in October.

329 Table 3: Correlation coefficients among variables for upstream sites (D1-D5)

			October			
			NO_3	DOC	$\delta^{18}O\text{-}NO_3$	$\delta^{15}N\text{-}NO_3$
	NO_3	Pearson Corr.	1	-0.01	-0.93	-0.39
	NO_3	p_value	--	0.99	0.07	0.61
	DOC	Pearson Corr.	-0.21	1	-0.03	0.34
April	DOC	p_value	0.74	--	0.97	0.66
	$\delta^{18}O\text{-}NO_3$	Pearson Corr.	-0.50	0.68	1	0.09
	$\delta^{18}O\text{-}NO_3$	p_value	0.50	0.32	--	0.91
	$\delta^{15}N\text{-}NO_3$	Pearson Corr.	0.31	0.75	0.65	1
	$\delta^{15}N\text{-}NO_3$	p_value	0.69	0.25	0.35	--

330

331 <Fig. 4 close to here>

332 <Fig. 5 close to here>

333 The PCA for upstream sites (D1-D5) in April and October campaigns (Fig. 5) showed about 90% of data
334 variability was explained by the first 2 components (axes). Statistically, these 2 first axes were sufficient
335 to represent the variability of the whole data set. In both periods, the first axis had high positive
336 loadings of NH_4 and $\delta^{18}O\text{-}NO_3$ and a high negative loading of NO_3. Axis 2 had high positive loadings of

337 δ^{15}N-NO_3 and DOC. The most noticeable difference between the 2 months is that DOC and δ^{15}N-NO_3
338 changed from high loadings in April to low, negative loadings in October as is demonstrated in their
339 distribution on axis 1.

340 **Partition of N sources**

341 <Fig. 6: Fractions of the different N-sources calculated for each site>

342 In general, the natural end members (soil/groundwater and Red River inputs) dominated (more than any
343 other anthropogenic end member sources) in the upstream (D1-D5) and downstream (D10-D11)
344 reaches. On the other hand, in the dry season, manure and sewage end member sources were more
345 dominant, particularly in the middle section of the DRB (representing more than >50% of total NO_3 at
346 D5-D9). In addition, D9 is located at the point of greatest agricultural impact, especially notable in the
347 fertilization and rainy periods of July (79±14%). As shown in Fig. 6, for all surveys, the proportion of
348 natural (soil/groundwater and Red River inflow sources) end member inputs to the DRB accounted for
349 not more than 50±23% of the total NO_3 concentrations in the river. Only in the rainy season and when
350 fertilizers were applied (July), did manure and sewage contributions account for a smaller fraction
351 (15±8%) than agricultural sources (45±10%). For other periods (April and October), anthropogenic
352 sources of NO_3 were greater contributors than agricultural sources to the DRB, which is unsurprising
353 given that the DRB is one of the most urbanized catchments in Vietnam.

354 The results of partition calculations demonstrated that chemical fertilizer was a main source for NO_3 in
355 Day River during the rainy season. Even during the non-fertilization period (October), fertilizer derived
356 NO_3 still accounted for 20±10% of nitrate sources. This number increased to 45±10% (mentioned above)
357 when fertilizer was applied during rainy season (July), while in the dry season only 15±13% of the river
358 NO_3 was derived from nitrified urea fertilizers.

Partition calculations for the downstream sites D10 and D11 showed that the Red River fractions of NO_3 constituted up to about 50±7% of the total NO_3 (Fig. 6).

Discussion

This manuscript aims to address two central questions, which include where the main sources of river NO_3 come from and what the dominant biogeochemical processes are which control the fate of NO_3 in the DRB. To address these questions, the Discussion is organized in two sections. The first is to examine our applied mixing model results to distinguish if agriculture (rice cultivation and their fertilizer sources) and/or urbanization (anthropogenic sources) are the main sources of NO_3 to the DRB. Our second direction is to correlate isotopic signatures with nitrate and carbon availability so as to estimate the loss (via denitrification and assimilation) and gain (via nitrification) of NO_3 in the DRB catchment and its streams. Our discussion aims to elucidate these points so as to ultimately propose plans for pollution detection, alleviation and better management practice in the catchment.

Sources of nitrate in the DRB

The weak positive correlation coefficient between $\delta^{15}N$ and $\delta^{18}O$ (R = 0.39 (p_value = 0.05); Fig. 4) indicates the absence of a simple mixing of sources along the DRB. Nor does it indicate that one single biological process is responsible for the nitrate content in this river network. Indeed, the clear evidence of multiple mixing is further demonstrated by the sharp change in water isotope compositions between sites D9 and D10, and further still between D10 and D11 (Fig. 2f). The first change in these signatures reflects a substantial mixing of waters at D10 with the Red River water, which is delivered to the site via the Dao River (Trinh et al., 2017) and the latter change (at D11) is due to mixing with sea water (with the site located only 3 km from the sea (Table 1)).

Overall, we conclude that the different seasonal surveys capture the dominance of varied N sources at different times of the year (refer to Fig. 4 and the partition calculations). For example, in April, when rain is limited, river water is dominated by manure and sewage derived NO_3 sources. This is a period of (1) limited discharge of chemical fertilizers from paddy fields to water ways and (2) a reduced input of naturally derived NO_3 from soil and groundwater sources (due to the drier climatic conditions). However, during the rainy season (July and October), manure and sewage sources become less dominant due to the increased input of N derived from natural, upstream sources. In addition, nitrified urea fertilizer plays an important role in regulating river nitrate concentrations in July (which is the dominant urea fertilization period), as indicated by a lower $\delta^{15}N$ signature than in other periods (Fig. 3b). While nitrate sources in the DRB appear to be dominated by manure and sewage in April, and chemical fertilizer in July, in October neither appear to be most important. Our partition calculation results represented in Fig. 6 also support the findings of Luu et al. (2012) that more than 50% of nutrient input to the RRD (of which the DRB is a sub-basin) is from anthropogenic activities.

Agricultural practices and their impacts on riverine NO_3 in the DRB

Variations in NO_3 stable isotope compositions in the DRB are similar to those in other watersheds (Battaglin et al., 2001, Chen et al., 2009, Lin et al., 2019). For instance, the fractionation effect observed for $\delta^{15}N\text{-}NO_3$ on the upper reaches of watersheds is often higher than the fractionation observed further downstream. This highlights the importance of the biogeochemical processes taking place in upstream reaches, accounting for these isotopic signatures. Furthermore, seasonal changes in $\delta^{15}N\text{-}NO_3$ signatures of the DRB are greater than the ranges observed along the upstream - downstream continuum, implying the importance of natural processes (i.e., rainfall and temperature) in generating greater changes in nitrate isotope ratios (point sources and non-point sources) along the river reach. Indeed, in the DRB where agricultural activities dominate and precipitation regimes are seasonal, such seasonal changes of

403 water and nitrate stable isotope signatures between wet and dry seasons and between planting and
404 harvesting periods, are displayed.

405 There are, on the other hand, some distinctive differences between the DRB and eutrophic river systems
406 elsewhere in the world. For instance, compared to other studies (Battaglin et al., 2001, Chen et al., 2009,
407 Lin et al., 2019), the present study (building on earlier work of Ta et al., 2016) is among the few
408 reporting $\delta^{15}N\text{-}NO_3$ values < 0 (Popescu et al., 2015; Vrzel et al., 2016). A rational explanation is that
409 urea characterized with depleted $\delta^{15}N$ is extensively used in the DRB and agriculture is the dominant
410 source of NO_3 in many parts of this system. In fact, synthetic urea fertilizers of low (negative) $\delta^{15}N$ were
411 reportedly used in paddy fields of the RRD (Ta et al., 2016; Saiki et al., 2019). In all surveys conducted in
412 this study, $\delta^{15}N$ at site D9 was always lower than the preceding upstream site (D8). We argue that this is
413 directly resulting from the large proportion of agricultural water which discharges from the Sat River at
414 site D9. As shown in Fig. 1, the Sat River irrigates and drains large paddy fields and wetlands in Ha Nam
415 and Nam Dinh Provinces. As a result, the composition of the Sat River should be (and is) characterized by
416 low $\delta^{15}N$. An implication of this finding is that there is a need to re-evaluate the application of fertilizer
417 to paddy fields in the DRB so as to moderate fertilizer application rates, especially during rainy seasons.
418 These arguments are also based on the partition calculation conducted in this study, which found that at
419 D9, during the rainy season and fertilization period, 79±14% of NO_3 in the river water is derived from
420 chemical fertilizer sources. If one takes into account the water discharge of c. 540 $m^3\ s^{-1}$ in this middle
421 section during the rainy season (Luu et al., 2010) and a concentration of NO_3 of 0.5 mg N L^{-1} at D9
422 (derived in this study), we can then estimate the amount of chemical N fertilizers discharging in DRB
423 during this period to be c. 18.66 t d^{-1}. Compared to data published elsewhere (e.g. Luu et al., 2012 argue
424 that total N delivered from DRB as about 30 t d^{-1}), this study shows how substantially large the impact
425 the chemical N fertilizer is to aquatic media (not only riverine but also coastal) in this region.

Manure and sewage NO_3 sources in the DRB

High values of river $\delta^{15}N$ signatures in the middle section of the DRB can be attributed to an increasing impact of domestic waste (manure and sewage) discharge, characterized with a high $\delta^{15}N$ (Bateman & Kelly 2007). Our partitioning calculation shows that the manure/sewage fraction reaches as high as 80% in this middle section (D6-D8) in April (the dry season) and in October (the rainy season) (Fig. 6). However, while the manure and sewage fraction and NO_3 concentration in April are about 1.5 and 2 times higher (respectively) than those values in October, the river discharge in April is only about one third of that in October. We see that there are therefore similar loads of manure and sewage NO_3 between the 2 surveys. In fact, Luu et al. (2010) also reported a seasonally unvarying flow of the main open-air sewer of the north-eastern part of the catchment (Hanoi Metropolis) which would further support our argument.

Using land use data and Material Flow Analysis, Do et al. (2014, 2019) estimated nitrogen loads in the DRB for the period of 2008 – 2010 and found that the Day River receives approximately 9600 t yr^{-1} of chemical N fertilizer and 12000 t yr^{-1} of anthropogenic induced organic N (all forms/species of N), respectively. The Day River therefore receives more anthropogenic organic N (e.g. manure, sewage or sludge) than chemical fertilizer N loading. Do et al. (2014) however were not able to provide a seasonal assessment of the changes between chemical and organic N inputs to the river. Here we show (Fig. 6) that the ratio between chemical fertilizer and anthropogenic organic NO_3 sources vary between about 0.3 in the dry season (April) and about 3.0 in the rainy and fertilization period (July). All our results therefore highlight (1) the impact of chemical fertilizer sources of NO_3 on the Day River and (2), more importantly, that there is an absence of seasonal variability in the anthropogenic sourced organic NO_3 end members in the DRB. The larger portion of organic NO_3 (in this case defined as manure and sewage), reflects the impact of urbanization and industrialization in the DRB.

Biogeochemical processing in the DRB

Nitrification processes in the DRB

Nitrate inputs into streams are generally derived from (1) atmospheric deposition, (2) soil/groundwater NO_3 leaching, (3) excessive application of nitrate fertilizers and (4) the nitrification of reduced N species (Kendall 1998). Based on our discussion in the preceding section, it is clear that (1) atmospheric deposition and (2) groundwater NO_3 leaching are minimal sources of NO_3 to the DRB, as is (3) excessive nitrate fertilizer application (Fig 4). In other words, we argue that NO_3 in the DRB is derived by the nitrification of reduced N species. This is highlighted by the seasonal analogue between $\delta^{18}O\text{-}H_2O$ and $\delta^{18}O\text{-}NO_3$, which is higher in the dry season and lower in the rainy season (Fig. 2f and 3a), as the *in situ* nitrified NO_3 will consist of one oxygen atom derived from water in its molecule.

Seasonally, our data suggest that nitrification is more dominant in the rainy season than the dry season and more visible at sites with larger agricultural input (e.g. site D9). This seasonal trend is further supported by Ta et al. (2016) for the Red River, who found a higher negative correlation between $\delta^{18}O\text{-}NO_3$ and $\ln(NO_3)$ in the rainy season (over the dry season) and concluded therefore that nitrification was more dominant during the former. This statement is corroborated by this study, where the correlation coefficient between $\delta^{18}O\text{-}NO_3$ and $\ln(NO_3)$ is -0.73 (p_value = 0.01, significantly correlated at p 0.05) in the October (wet season) sampling. Meanwhile in April, the dry season, the correlation coefficient is lower and insignificant (= -0.47, p_value = 0.17, insignificantly correlated at p 0.05).

Spatially, the downstream-depleted tendency of $\delta^{18}O\text{-}NO_3$ (except for sites D10 and D11 where water is strongly mixed with the Red River water and/or marine water (Trinh et al., 2017 and concluded herein)) may reflect an increasing contribution of in-stream nitrified NO_3. The prevalence of nitrification in the DRB is evident when examining the nitrate isotopic signatures at site D9, the point of the greatest agricultural impact (the Sat River inflow). Here isotope signatures, especially $\delta^{18}O\text{-}NO_3$, were particularly

lower than at all other sites (Fig. 3a). While the low $\delta^{15}N$ is concluded to be of a chemical fertilizer origin, the low $\delta^{18}O\text{-}NO_3$ compositions could only be a result of nitrification. Indeed, recent studies (e.g. Casciotti et al. 2007; Casciotti et al., 2010; Buchwald & Casciotti, 2010) have presented oxygen isotopic exchange and fractionation during nitrification to form NO_3, with $\delta^{18}O\text{-}NO_3$ falling between -8.3 and -0.7‰ of the ocean water ($\delta^{18}O\text{-}H_2O_{,VSMOW}$). By applying the formulas and fractionation coefficients reported in those studies (refer to appendix) to our case study, where $\delta^{18}O\text{-}H_2O$ of river water signatures range between -8 and -4‰ (Fig. 2f), the $\delta^{18}O\text{-}NO_3$ composition of nitrified NO_3 would be between -10.4 and -7.6‰. Comparing $\delta^{18}O\text{-}NO_3$ signatures at D9 (which are between -7.07 and -2.01‰ for all three sampling periods, Fig. 3a), we conclude that NO_3 at site D9 is largely a result of the nitrification of urea fertilizers and that isotope enrichment (via assimilation) is minimal (Panno et al., 2006). Rather, we argue that the more positive $\delta^{18}O\text{-}NO_3$ values at sites D9 than the ones calculated for nitrified urea fertilizer sources alone, are due to mixing with other nitrate sources (of other nitrate sources of more positive isotope values) and/or fractionation (NO_3 delivered to site D9 has already been fractionated (e.g. denitrification) to increase its signature).

The PCA applied to upstream sites (D1-D5) has shown a similarity between DOC and $\delta^{15}N\text{-}NO_3$ variables in both April and October which we conclude signifies that NO_3 is predominantly derived from soil and domestic organic matter. The opposite positioning of NO_3 and NH_4 vectors for these upstream sites (Fig. 5) also implies that NO_3 is sourced from NH_4 and NH_4 in turn, results from a degradation of organic matter. These PCA results confirm those of the partition calculation which also show a dominance of soil and sewage/manure sources in upstream sites (Fig. 6a,c).

Denitrification and biological assimilation

Overall, the weak positive correlation between $\delta^{15}N$ and $\delta^{18}O$ signatures (R = 0.39 (p_value = 0.05); Fig. 4) represents isotopic enrichment in the DRB. The isotopic enrichment is likely a result of denitrification

and/or biological assimilation since these processes fractionate nitrate nitrogen and oxygen isotopes equally, leaving behind nitrate that is enriched in both ^{15}N and ^{18}O (Granger et al. 2004, 2008).

Studies have shown that stream systems are particularly efficient at removing and retaining excess nitrogen (N) (Seitzinger et al., 2006) with headwater and mid-network streams being the most effective in the regulation of downstream N exports (Peterson et al., 2001; Alexander et al., 2000; Mulholland et al., 2008). Characteristics of these headwater and mid-network streams is the higher contact (exchange potential) between water and sediment interfaces than in downstream reaches [Anderson et al., 2005], especially during periods of low discharge (Wondzell, 2011). This pattern is particularly evident for the DRB since river flow in the upper reaches of the Day River (sites D1 and D2; Fig. 2f) are lower, resembling a lentic system and thereby providing an environment more conducive to denitrification. Fig 5 also supports these statements, due to strong positive association of $\delta^{18}O\text{-}NO_3$ and NH_4 with axis 1. The opposite relationship with NO_3 along axis 1, suggests a nitrification-denitrification process is at play, capturing the conversion of N species at sites D1-D5 between oxidized (NO_3) and reduced N (NH_4). This very upstream section is also an urbanized area and part of the Hanoi Metropolis (Fig. 1). Indeed statistical tests run on data from the upstream sites have confirmed (1) the dominance of organic matter mineralized and nitrified NO_3 (Fig. 5 and discussed above) and more importantly (2) the increased denitrification during the dry season which is demonstrated by the strong association between $\delta^{15}N$ and $\delta^{18}O$ along axis 1 (Fig. 5a) (acting as a nitrification-denitrification scale) and the positive correlation coefficient between the 2 isotopes (= 0.65, p_value =_0.34).

The higher signatures seen and the more pronounced increasing trend of $\delta^{15}N\text{-}NO_3$ in upstream samples (sites D1-D5) in April (Fig. 3b) also suggests a greater denitrification of NO_3 sources. The greater degree of denitrification may indicate relatively longer residence times and more intensified biological activities in these parts of the DRB (as discussed above) during the dry period. Compared to isotopic data

obtained in temperate, higher latitude climates, where summer and autumn are seasons of stronger biological activity in upstream regions (e.g. Panno et al., 2006) our data indicates an opposite seasonal change, for denitrification. The difference is because in the DRB the temperature rarely decreases to below 10^{o}C, a condition which would limit biological activity (including plant growth) and denitrification. Even during the monsoon rainy season, when N soil leaching may increase, the intense precipitation dilutes these nutrients and carbon species (indicated by low DOC concentrations; Fig. 2e) to lessen biological activity as well.

Another line of evidence for denitrification occurring at polluted water sites in the DRB is shown via the partition calculation. Negative fractions of chemical fertilizer or manure/sewage end members at sites D1 and D2 (the most upstream sections), where water flows slowly, and site D6, where the Day River receives urban wastewater brought in by the Nhue River (Fig. 1), reflect some strong isotope fractionation. Mathematically, such a negative trend is found if the data points are outside of the end member matrix. This may occur if, (1) by some means, the isotopic fractionation of NO_3 continues substantially downstream (for this case, biological activities will drive fractionation effects to account for the extreme isotopic compositions) or (2) an improper selection of end-member values. When considering option 2, we cannot rule out the possibility of having improperly selected end-member source values, which would result in negative values. As shown in Table 2, the source values were selected based on a limited number of analytical results or derived from the literature. While future studies should enhance this analytical gap for the DRB, so as to further validate our estimations, we feel confident that our calculations remain valid for this study. As such, we explain that such negative values are due to in-stream isotopic fractionation. In a still water body, that receives a large amount of domestic wastewater (indicated by high DOC concentrations as shown in Fig. 2e), respiration and biodegradation processes would help drive the enrichment of ^{15}N organic N (Kendall et al., 2007) and ^{18}O dissolved oxygen (Quay et al., 1995). Our monthly surveys of water quality show a hypoxic state during

542 dry periods (results not shown). As a consequence, NO_3 produced in such a system should be
543 characterized by elevated $\delta^{15}N\text{-}NO_3$ and $\delta^{18}O\text{-}NO_3$ signatures. Furthermore, as denitrification will likely
544 take place in this respiration dominated aquatic medium, NO_3 will be characterized with higher isotopic
545 signatures (Site 1 in Fig. 3). To sum up, in heterotrophic ecosystems, nitrification takes place in an
546 elevated $\delta^{18}O\text{-}O_2$ media, which will produce NO_3 characterized by a high $\delta^{18}O\text{-}NO_3$ composition.
547 Following nitrification in such a heterotrophic system, denitrification will lead to a higher $\delta^{18}O\text{-}NO_3$
548 signature of the remaining NO_3 pool so that, nitrate isotope compositions will plot outside of the end-
549 member matrix.

550 Another important observation from the spatio-temporal assessment of in-stream denitrification is
551 whether this has triggered localized within stream hypoxia or anoxia. As denitrification is a reduction
552 process which is intense in parts of the DRB, it is possible that water at certain depth in the river water
553 column has equally been altered to less oxic conditions, which has implications on within stream aquatic
554 ecosystem health. In fact, previous studies on several streams/rivers in the DRB have shown that the
555 rivers running through urban areas are transformed into, and actually function as, open air sewers (Duc
556 et al., 2007; Trinh et al., 2012). At several upstream sites in the DRB where urbanization has increased
557 over the last 20 years, domestic wastewater has notably increased its proportion in the catchment
558 water discharge, which has subsequently augmented the amount of biogeochemical processing which
559 would otherwise not have taken place in surface waters (e.g. denitrification, methane production),
560 thereby deteriorating the local environment.

561 **Carbon and NO_3 variability in the DRB**

562 Discussions in the precedent sub-sections have pointed to a reality that in tropical aquatic systems,
563 carbon availability (which is related to biodegradable organic matter) plays an important role in NO_3
564 variability. Many authors have reported the relationship between carbon availability and

denitrification/assimilation in streams and rivers (Baker and Vervier, 2004; Zarnetske et al., 2011; Johnson et al., 2012). For instance, Baker and Vervier (2004) highlight that rates of denitrification were driven by the concentration of low molecular weight organic acids, derived from the decomposition of soil organic matter. In particular, DOC availability and river-floodplain connectivity were important factors influencing this process. Similarly, others argued that denitrification in anaerobic portions of the hyporheic zone is limited by labile DOC supply (Zarnetske et al. 2011) and that DOC enrichment in the water column will cause N assimilation to increase (Johnson et al. 2012). As discussed above, our data have highlighted that carbon availability (DOC) has an impact on the NO_3 variability in the DRB, especially in the upstream sites during the dry period. As demonstrated in Fig 5, DOC is strongly associated with $\delta^{15}N$ and $\delta^{18}O$ at the upstream sites of the DRB. This is further corroborated by correlation coefficients of $\delta^{18}O\text{-}NO_3$ – $\delta^{15}N\text{-}NO_3$, $\delta^{18}O\text{-}NO_3$ – DOC, and $\delta^{15}N\text{-}NO_3$ – DOC which are respectively 0.65 (p_value = 0.35), 0.68 (p_value = 0.32) and 0.75 (p_value = 0.25). These data together imply that DOC plays a prominent role in the denitrification process of the DRB in the dry season.

Conclusion

This study highlights the effectiveness of applying stable isotope approaches such as water and dual NO_3, to assess the provenance and biogeochemistry of an aquatic system impacted by multiple pollution sources. With the use of nitrate isotope data, we show how biological activities drive the isotopic compositions of nitrate in the DRB, Vietnam; these processes include nitrification of urea, NH_4 in autotrophic and heterotrophic media, and denitrification.

We identify 4 different sources of NO_3 in the DRB, with differing importance along the river course. Inorganic urea fertilizer is a major source (particularly at site D9), along with urban sewage, showing a clear impact especially the downstream sections, after the confluence with the Nhue River (at site D6). Indeed, this study shows how strongly anthropogenic activities have impacted the Day River system. In

588 the middle section, after the confluence with the Nhue River, the proportion of natural inputs
589 (soil/ground and upstream Red River inflow sources) of NO_3 rarely contribute more than 50%. Rather,
590 the high proportion of NO_3 deriving from anthropogenic activities in the DRB is apparent. Our study
591 highlights that there is a need to re-evaluate the application of inorganic fertilizers to paddy fields in the
592 DRB region, so as to moderate excessive application. This is particularly important when fertilization
593 practices are taking place in the rainy season, where rapid and large scale delivery of NO_3 (derived from
594 urea end-member sources) is demonstrated.

595 ## Acknowledgement

596 This work was supported by the RCUK-NAFOSTED [grant numbers NE/P014577/1]; and the NAFOSTED
597 [grant number 105.08-2014.26]. Stable isotope analysis was performed as part of the IAEA-CRP program
598 'Isotopes to Study Nitrogen Pollution and Eutrophication of Rivers and Lakes – F32007'. This paper is
599 written with a financial support from the Graduate School of Science and Technology, Vietnam Academy
600 of Science and Technology (GUST.STS.ĐT2017-ST02).

601 ## References

602 Amberger, A. & Schmidt, H.-L., 1987. Natürliche Isotopengehalte von Nitrat als Indikatoren für dessen
603 Herkunft. *Geochimica et Cosmochimica Acta,* Volume 51, pp. 2699-2705.

604 Baker, M. A. & Vervier, P., 2004. Hydrological variability, organic matter supply and denitrification in the
605 Garonne River ecosystem. *Freshwater Biology,* 49(2), p. 181–190.

606 Bateman, A. S. & Kelly, S. D., 2007. Fertilizer nitrogen isotope signatures. *Isotopes in Environmental and*
607 *Health Studies,* Volume 43, pp. 237-247.

608 Battaglin, W. et al., 2001. Chemical and isotopic evidence of nitrogen transformation in the Mississippi
609 River, 1997--98.. *Hydrological Processes,* Volume 15, pp. 1285-1300.

610 Buchwald, C. & Casciotti, K. L., 2010. Oxygen isotopic fractionation and exchange during bacterial nitrite
611 oxidation. *Limnology and Oceanography,* 55(3), pp. 1064-1074.

612 Burns, D. A., Boyer, E. W., Elliott, E. M. & Kendall, C., 2009. Sources and transformations of nitrate from
613 streams draining varying land uses: evidence from dual isotope analysis.. *Journal of environmental*
614 *quality,* 5, 38(3), pp. 1149-59.

615 Burns, D. A. & Kendall, C., 2002. Analysis of δ15N and δ18O to differentiate NO3− sources in runoff at
616 two watersheds in the Catskill Mountains of New York. *Water resource research,* 38(5), pp. 9-1-9-11.

617 Casciotti, K. et al., 2007. Oxygen isotopes in nitrite: Analysis, calibration and equilibration. *Analytical*
618 *Chemistry,* Volume 79, p. 2427–2436.

619 Casciotti, K., McIlvin, M. R. & Buchwald, C., 2010. Oxygen isotopic fractionation and exchange during
620 bacterial ammonia oxidation. *Limnology and Oceanography,* 55(3), pp. 753-762.

621 Chen, F., Jia, G. & Chen, J., 2009. Nitrate sources and watershed denitrification inferred from nitrate dual
622 isotopes in the Beijiang River, south China. . *Biogeochemistry ,* Volume 94, pp. 163-174.

623 Clesceri, L. S., Greenberg, A. E. & Eaton, A. D., 1998. *Standard Methods for the Examination of Water*
624 *and Wastewater, 20th Edition.* s.l.:APHA American Public Health Association.

625 Coplen, T. B. & Wassenaar, L. I., 2015. LIMS for Lasers 2015 for achieving long-term accuracy and
626 precision of δ2H, δ17O, and δ18O of waters using laser absorption spectrometry. *Rapid Communications*
627 *in Mass Spectrometry,* Volume 29, pp. 2122-2130.

628 DARD-Hanoi, 2009. *Guidance of chemical fertilizers utilization in Chuong My district, Ha Noi capital (in*
629 *Vietnamese) ,* s.l.: Department of Agriculture and Rural Development—Hanoi .

630 DARD-Namdinh, 2011. *Guidance of chemical fertilizers utilization in Vu Ban district, Nam Dinh province*
631 *(in Vietnamese),* s.l.: Department of Agriculture and Rural Development— Nam Dinh.

632 Do, N. T., Trinh, D. A. & Nishida, K., 2014. Modification of uncertainty analysis in adapted material flow
633 analysis: Case study of nitrogen flows in the Day-Nhue River Basin, Vietnam. *Resources, Conservation &*
634 *Recycling,* Volume 88, pp. 67-75.

635 Do, T. N. & Nishida, K., 2014. A nitrogen cycle model in paddy fields to improve material flow analysis:
636 the Day-Nhue River Basin case study. *Nutrient Cycling in Agroecosystems,* 01 11, Volume 100, pp. 215-
637 226.

638 Do, T. N., Tran, B. V., Trinh, A. D. & Kei, K. N., 2019. Quantification of nitrogen load in a regulated river
639 system in Vietnam by material flow analysis. *Journal of Material Cycles and Waste Management,* 21(4),
640 p. 974–98.

641 Duc, T. A. et al., 2007. Experimental investigation and modelling approach of the impact of urban
642 wastewater on a tropical river; a case study of the Nhue River, Hanoi, Viet Nam. *Journal of Hydrology,* 2,
643 Volume 334, pp. 347-358.

644 Galloway, J. N. et al., 2004. Nitrogen Cycles: Past, Present, and Future. *Biogeochemistry,* 01 9, Volume
645 70, pp. 153-226.

646 Giap, T. V. et al., 2007. *Study Of Isotopic Technical Application To Estimate Origin Of Nitrogen*
647 *Composition Of Groundwater In Hanoi Area,* Viet Nam: s.n.

GSO, 2014. *Report on the census of rural, agriculture and aquaculture ,* s.l.: Vietnam General Statistics Office.

GSO, 2016. *Statistical Year Book of Ha Noi, Ha Nam, Nam Dinh, Ninh Binh, Hoa Binh province,* s.l.: Vietnam General Statistics Office.

Hanh, P. T. M. et al., 2010. Anthropogenic influence on surface water quality of the Nhue and Day sub-river systems in Vietnam. *Environmental Geochemistry and Health,* 01 6, Volume 32, pp. 227-236.

Johnson, L. T., Royer, T. V., Edgerton, J. M. & Leff, L. G., 2012. Manipulation of the Dissolved Organic Carbon Pool in an Agricultural Stream: Responses in Microbial Community Structure, Denitrification, and Assimilatory Nitrogen Uptake.. *Ecosystems,* Volume 15, p. 1027–1038.

Kendall, C., 1998. Chapter 16 - Tracing Nitrogen Sources and Cycling in Catchments. In: C. KENDALL & J. J. McDONNELL, eds. *Isotope Tracers in Catchment Hydrology.* Amsterdam: Elsevier, pp. 519-576.

Kendall, C., Elliott, E. M. & Wankel, S. D., 2007. Tracing anthropogenic inputs of nitrogen to ecosystems. In: R. Robert Michener & K. Lajtha, eds. *Stable Isotopes in Ecology and Environmental Science, 2nd Edition.* Oxford: Wiley-Blackwell, p. 594.

Kurosawa, K. et al., 2004. Monitoring of Inorganic Nitrogen Levels in the Surface and Ground Water of the Red River Delta, Northern Vietnam. *Communications in Soil Science and Plant Analysis,* Volume 35, pp. 1645-1662.

Kurosawa, K. et al., 2006. Temporal and Spatial Variations of Inorganic Nitrogen Levels in Surface and Groundwater Around Hanoi, Vietnam. *Communications in Soil Science and Plant Analysis,* 3, Volume 37, pp. 403-415.

668 Lin, J. et al., 2019. Seasonality of nitrate sources and isotopic composition in the Upper Illinois River.
669 *Journal of Hydrology,* Volume 568, pp. 849-861.

670 Luu, T. N. M. et al., 2012. N, P, Si budgets for the Red River Delta (northern Vietnam): how the delta
671 affects river nutrient delivery to the sea. *Biogeochemistry,* 01 2, Volume 107, pp. 241-259.

672 Luu, T. N. M. et al., 2010. Hydrological regime and water budget of the Red River Delta (Northern
673 Vietnam). *Journal of Asian Earth Sciences,* Volume 37, pp. 219-228.

674 MARD, 2008. *Guidelines of fertilizers application for rice,* s.l.: Ministry of Agriculture and Rural
675 Development, Vietnam.

676 McIlvin, M. R. & Altabet, M. A., 2005. Chemical Conversion of Nitrate and Nitrite to Nitrous Oxide for
677 Nitrogen and Oxygen Isotopic Analysis in Freshwater and Seawater. *Analytical Chemistry,* Volume 77, pp.
678 5589-5595.

679 Michalski, G., Kolanowski, M. & Riha, K. M., 2015. Oxygen and nitrogen isotopic composition of nitrate in
680 commercial fertilizers, nitric acid, and reagent salts. *Isotopes in Environmental and Health Studies,*
681 Volume 51, pp. 382-391.

682 MONRE, 2006. *State of Environment in Vietnam,* s.l.: Ministry of Natural Resources and Environment,
683 Vietnam.

684 Panno, S., Hackley, K., Kelly, W. & Hwang, H., 2006. Isotopic evidence of nitrate sources and
685 denitrification in the Mississippi River, Illinois. *journal of environmental quality,* 35(2), pp. 495-504.

686 Popescu, R. et al., 2015. Using stable isotopes in tracing contaminant sources in an industrial area: A
687 case study on the hydrological basin of the Olt River, Romania. *Science of The Total Environment,*
688 Volume 533, pp. 17-23.

689 Quay, P. D. et al., 1995. The 18O:16O of dissolved oxygen in rivers and lakes in the Amazon Basin:
690 Determining the ratio of respiration to photosynthesis rates in freshwaters. *Limnology and*
691 *Oceanography,* Volume 40, pp. 718-729.

692 Quynh, L. T. P. et al., 2005. Nutrient (N, P) budgets for the Red River basin (Vietnam and China). *Global*
693 *Biogeochemical Cycles,* Volume 19.

694 Saiki, M., Do, T. N., Cao, T. T. H. & Nishida, K., 2019. *Temporal Variation of Stable Isotope Values For*
695 *Dissolved Nitrogen Compounds in Paddy Water Environment.* Ha Long, Vietnam, Vietnam Atomic Energy
696 Institute.

697 Seitzinger, S. et al., 2006. Denitrification across landscapes and waterscapes: a synthesis. *Ecological*
698 *Applications,* 16((6)), pp. 2064-2090.

699 Ta, T. T. et al., 2016. Interpretation of anthropogenic impacts (agriculture and urbanization) on tropical
700 deltaic river network through the spatio-temporal variation of stable (N, O) isotopes of NO−3. *Isotopes*
701 *in Environmental and Health Studies,* Volume 52, pp. 487-497.

702 Thibodeau, B., Hélie, J.-F. & Lehmann, M., 2013. Variations of the nitrate isotopic composition in the St.
703 Lawrence River caused by seasonal changes in atmospheric nitrogen inputs. 3.Volume 115.

704 Trinh, A. D., Meysman, F., Rochelle-Newall, E. & Bonnet, M. P., 2012. Quantification of sediment-water
705 interactions in a polluted tropical river through biogeochemical modeling. *Global Biogeochemical Cycles,*
706 Volume 26.

707 Trinh, D. A., Luu, M. T. N. & Le, Q. T. P., 2017. Use of stable isotopes to understand run-off generation
708 processes in the Red River Delta. *Hydrological Processes,* Volume 31, pp. 3827-3843.

709 Turner, R., Rabalais, N., Justic, D. & Dortch, Q., 2003. Global patterns of dissolved N, P and Si in large
710 rivers. *Biogeochemistry ,* 64(3), pp. 297-317.

711 Vrzel, J. et al., 2016. Determination of the sources of nitrate and the microbiological sources of pollution
712 in the Sava River Basin,. *Science of The Total Environment,* Volume 573, pp. 1460-1471.

713 Wankel, S., Kendall, C., Francis, C. & Paytan, A., 2006. Nitrogen sources and cycling in the San Francisco
714 Bay Estuary: A nitrate dual isotopic composition approach. *Limnology and Oceanography,* 51(4), p.
715 1654–1664.

716 Wassenaar, L. I., Coplen, T. B. & Aggarwal, P. K., 2014. Approaches for Achieving Long-Term Accuracy
717 and Precision of δ18O and δ2H for Waters Analyzed using Laser Absorption Spectrometers.
718 *Environmental Science & Technology,* Volume 48, pp. 1123-1131.

719 Widory, D. et al., 2013. Improving the management of nitrate pollution in water by the use of isotope
720 monitoring: the δ15N, δ18O and δ11B triptych. *Isotopes in Environmental and Health Studies,* Volume
721 49, pp. 29-47.

722 Zarnetske, J. P., Haggerty, R., Wondzell, S. M. & Baker, M. A., 2011. Labile dissolved organic carbon
723 supply limits hyporheic denitrification. *Journal of Geophysical Research ,* 114(G4).

724 Figure captions

725 Fig. 1: Map of Day River Basin and the sampling sites of this study.

726 Fig. 2: Concentrations of N species, DOC, and water stable isotopes ($\delta^{18}O\text{-}H_2O$) at different sampling
727 sites; April, July, and October are respectively the dry and fertilization period, rainy and fertilization
728 period, and rainy and non-fertilization period.

729 Fig. 3: Variation of nitrate stable isotopes (δ^{15}N-NO_3 and δ^{18}O-NO_3); April, July, and October are
730 respectively the dry and fertilization period, rainy and fertilization period, and rainy and non-fertilization
731 period.

732 Fig. 4: Crossplot of analytical δ^{15}N-NO_3 and δ^{18}O-NO_3 and the mixing model end member compositions;
733 2-tailed arrows in the horizontal axis represent the ranges of δ^{15}N-NO_3 if NO_3 is dominated by either
734 urea or manure/sewage.

735 Fig. 5: PCA for the upstream sites (D1-D5) in (a) April (b) and October

736 Fig. 6: Fractions of the different N-sources calculated for each site; Chem.Fert: chemical fertilizers (urea)
737 source, Man.Sew: sewage and manure source, Soil.Groun: soil and groundwater sources, Red.River:
738 inputs from the Red River

Appendix: Calculation of $\delta^{18}O$-NO_3 based on water oxygen and dissolved oxygen isotopes

Nitrification occurs as a two-step process whereby ammonia is first converted to nitrite and the produced nitrite is then converted to nitrate. During the bacterial nitrification process, the biogeochemical sources of oxygen atoms are dioxygen (O_2) and water (H_2O). O_2 is incorporated during the oxidation of ammonia to hydroxylamine (NH_2OH), while H_2O is incorporated during the oxidation of both hydroxylamine to nitrite and nitrite to nitrate. While the ratio of 1:2 oxygen atoms from O_2 and H_2O implied by these observations is commonly used to interpret the oxygen isotopic content of nitrate derived from bacterial nitrification (Kendall 1998; Burns and Kendall 2002; Wankel et al. 2006), the utilization of this ratio involves the assumptions that exchange and fractionation of oxygen isotopes during nitrification are minimal. Recent works (e.g. Casciotti et al. 2007; Casciotti et al., 2010; Buchwald and Casciotti, 2010) have presented oxygen isotopic exchange and fractionation during nitrification. In general, during bacterial ammonia oxidation, the produced $\delta^{18}O$-NO_2 is computed as:

$$\delta^{18}O_{NO_2} = \left[\frac{1}{2}(1 + x_{AOB})\right]\left(\delta^{18}O_{H_2O}\right) + \frac{1}{2}\left(\delta^{18}O_{O_2} - \varepsilon_{k,O_2} - \varepsilon_{k,H_2O,1}\right) + \left(\varepsilon_{eq}\right)\left(x_{AOB}\right) \quad (1)$$

In which χ_{AOB}, $\varepsilon_{k,O2,}$ $\varepsilon_{k,H2O,1}$, ε_{eq}, are respectively the fraction of nitrite oxygen atoms that have equilibrated with H_2O during ammonia oxidation, the kinetic isotope effect for O_2 incorporation, the kinetic isotope effect for H_2O incorporation by hydroxylamine oxidoreductase, and the equilibrium isotope effect for nitrite equilibration with H_2O.

Then, during bacterial nitrite oxidation, $\delta^{18}O$-NO_3 is estimated as (exchange of oxygen atoms between nitrite and water is minimal; Buchwald & Casciotti, 2010):

$$\delta^{18}O_{NO_3} = \frac{2}{3}\delta^{18}O_{NO_2} + \frac{1}{3}\left(\delta^{18}O_{H_2O} - \varepsilon_{k,H_2O,2}\right) \quad (2)$$

760 Whereas $\varepsilon_{k,H2O,2}$ is the kinetic isotope effect for water incorporation by nitrite oxidoreductase.

761 Literature review has shown that χ_{AOB}, $\varepsilon_{k,O2}+\varepsilon_{k,H2O,1}$, ε_{eq}, and $\varepsilon_{k,H2O,2}$ are respectively +0.15±0.1‰,
762 +26.3±7.7‰, +14‰, and +15.5±3.8‰ (Casciotti et al. 2007; Casciotti et al., 2010; Buchwald & Casciotti,
763 2010).

764

Figure 1

Click here to access/download;Figure;map.jpg

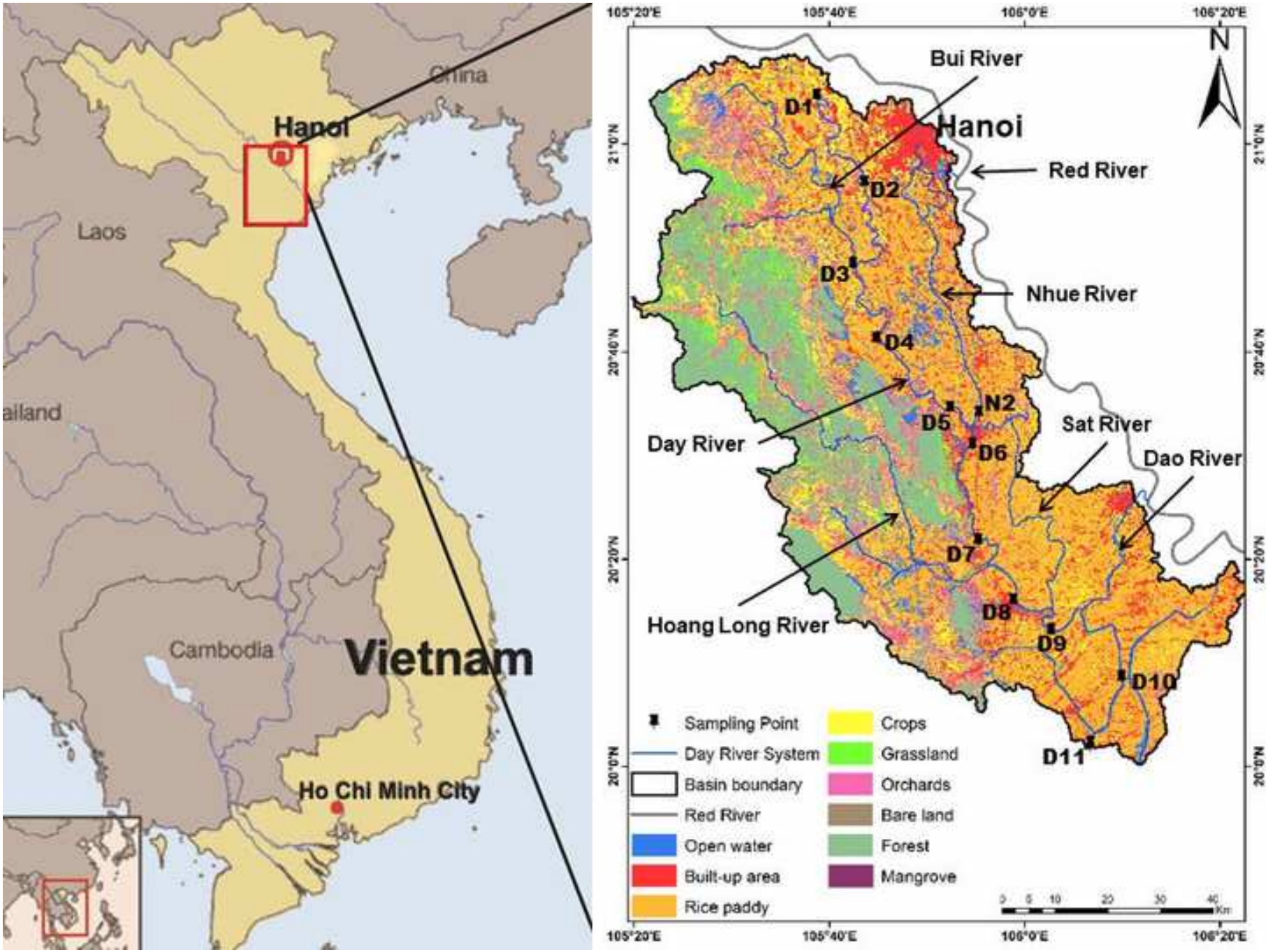

Figure 2a

Click here to access/download;Figure;Fig. 2a.BMP

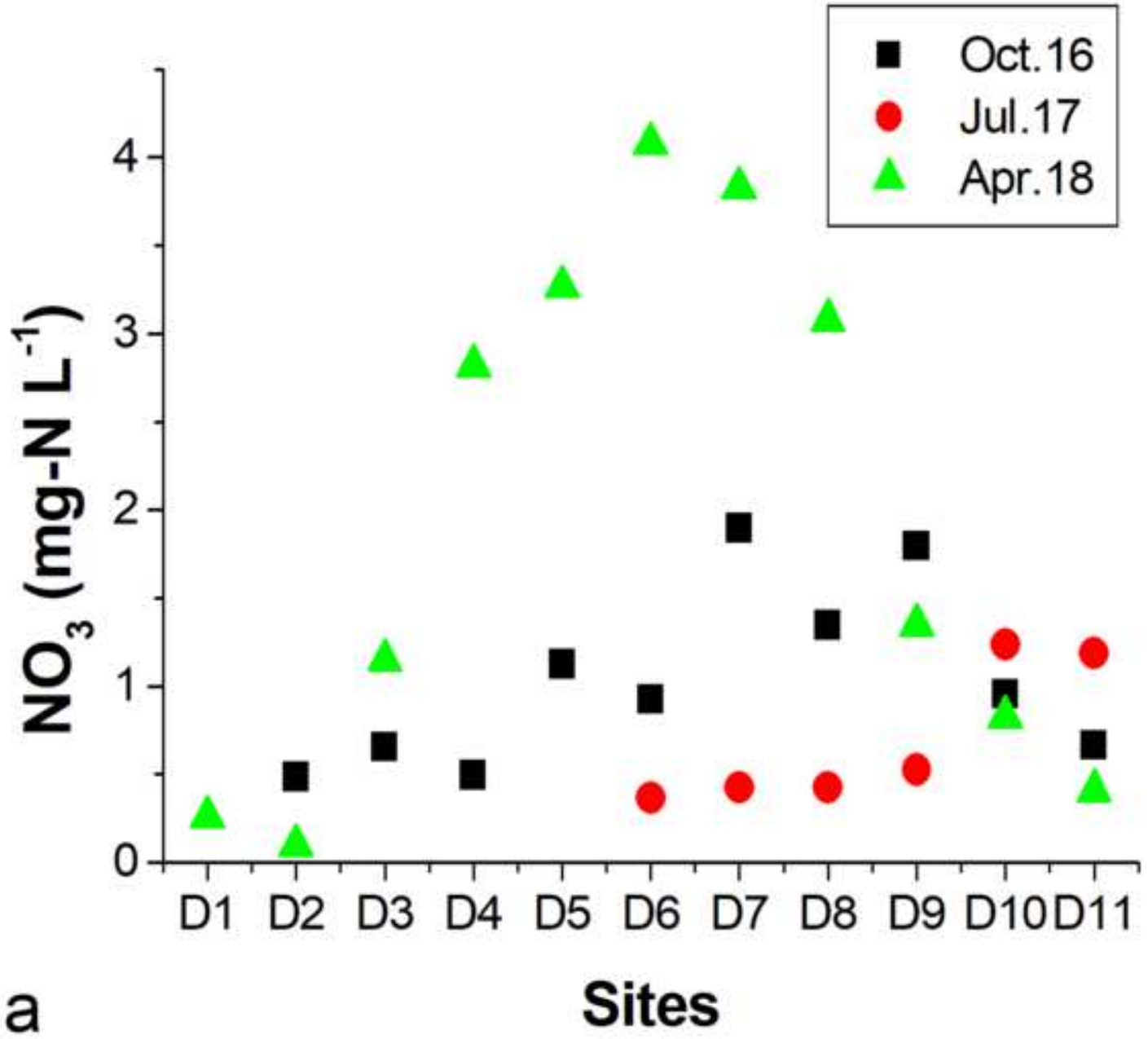

Figure 2b

Click here to access/download;Figure;Fig. 2b.BMP

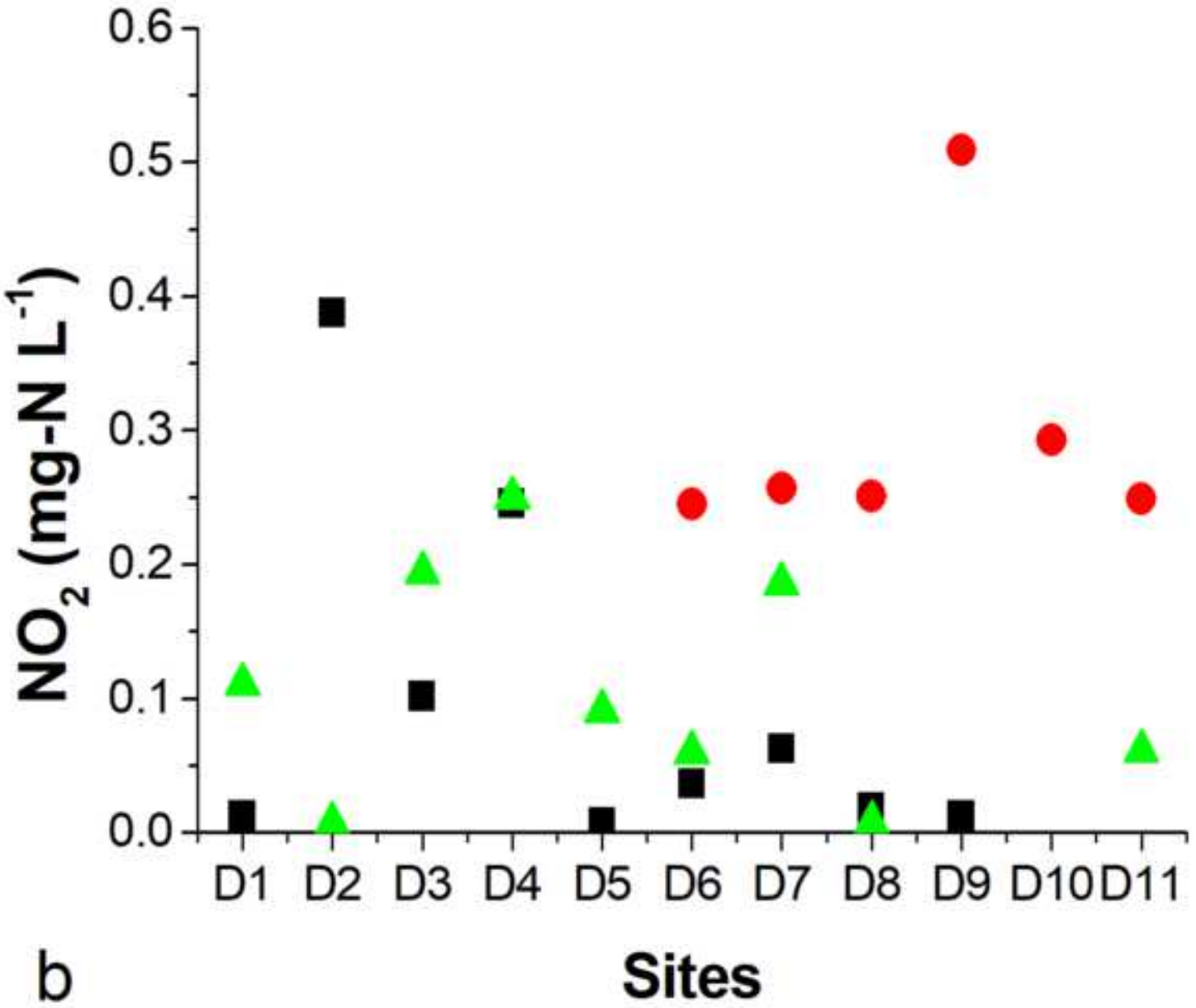

Figure 2c

Click here to access/download;Figure;Fig. 2c.BMP

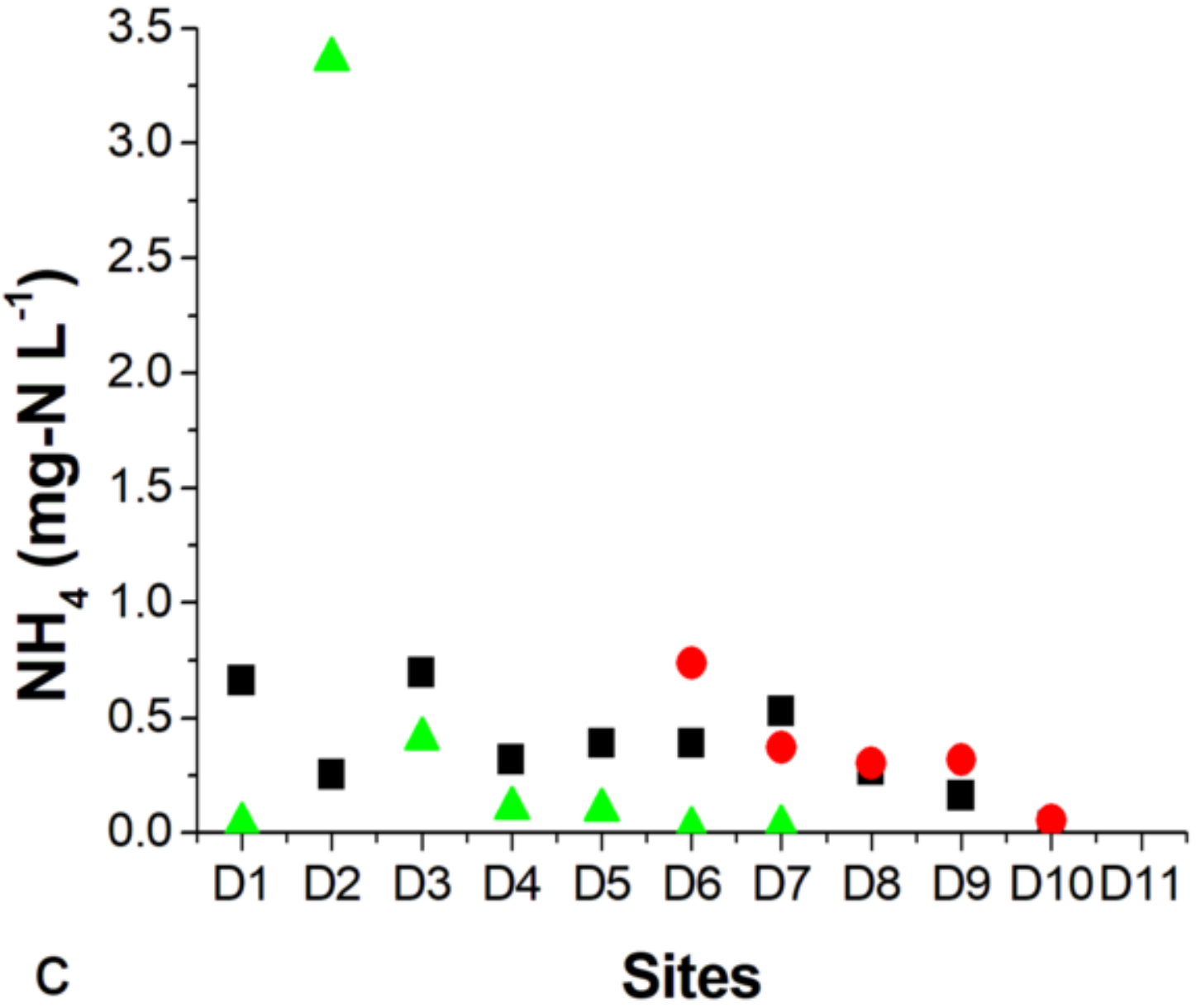

Figure 2d

Click here to access/download;Figure;Fig. 2d.BMP

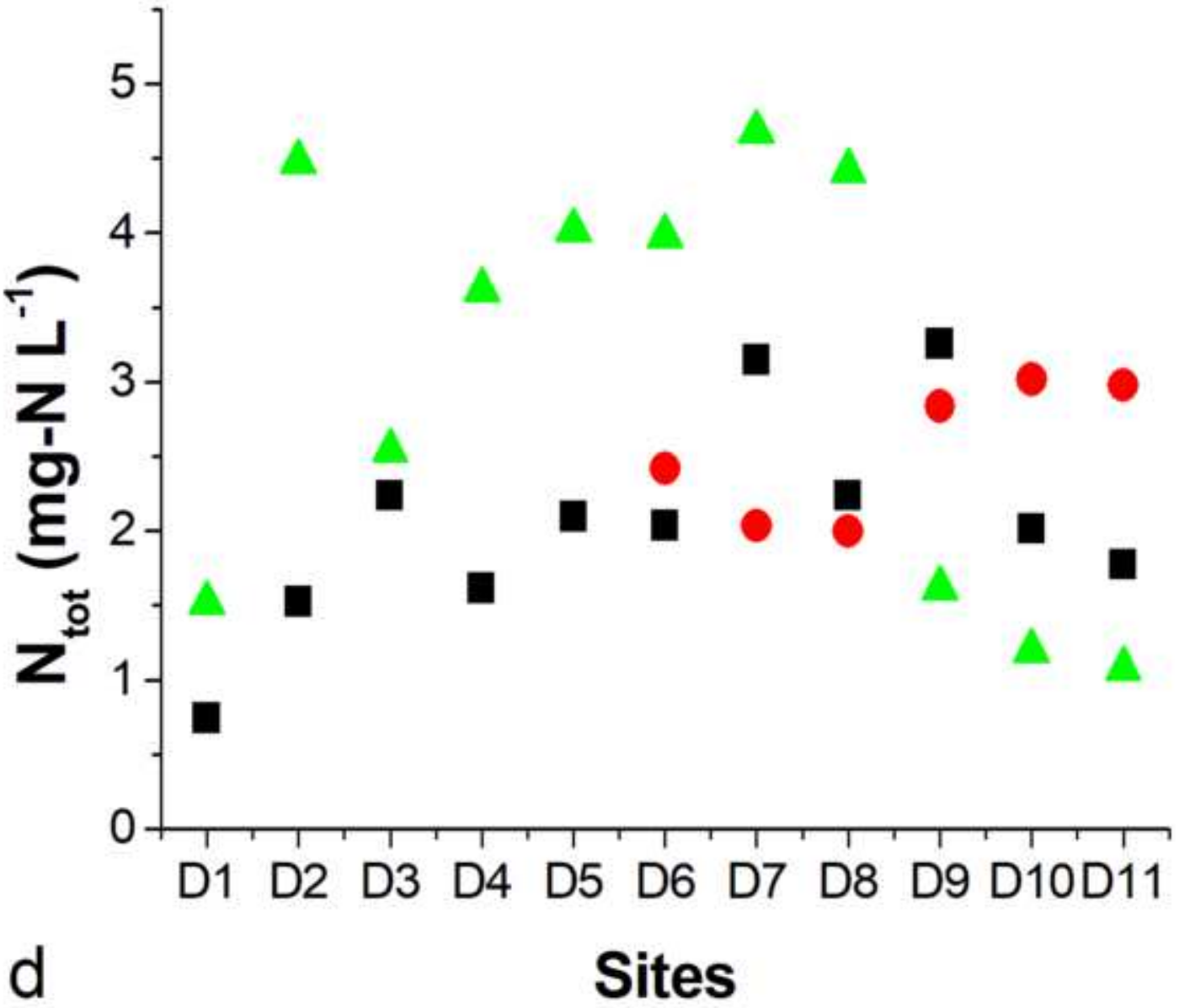

Figure 2e

Click here to access/download;Figure;Fig. 2e.BMP

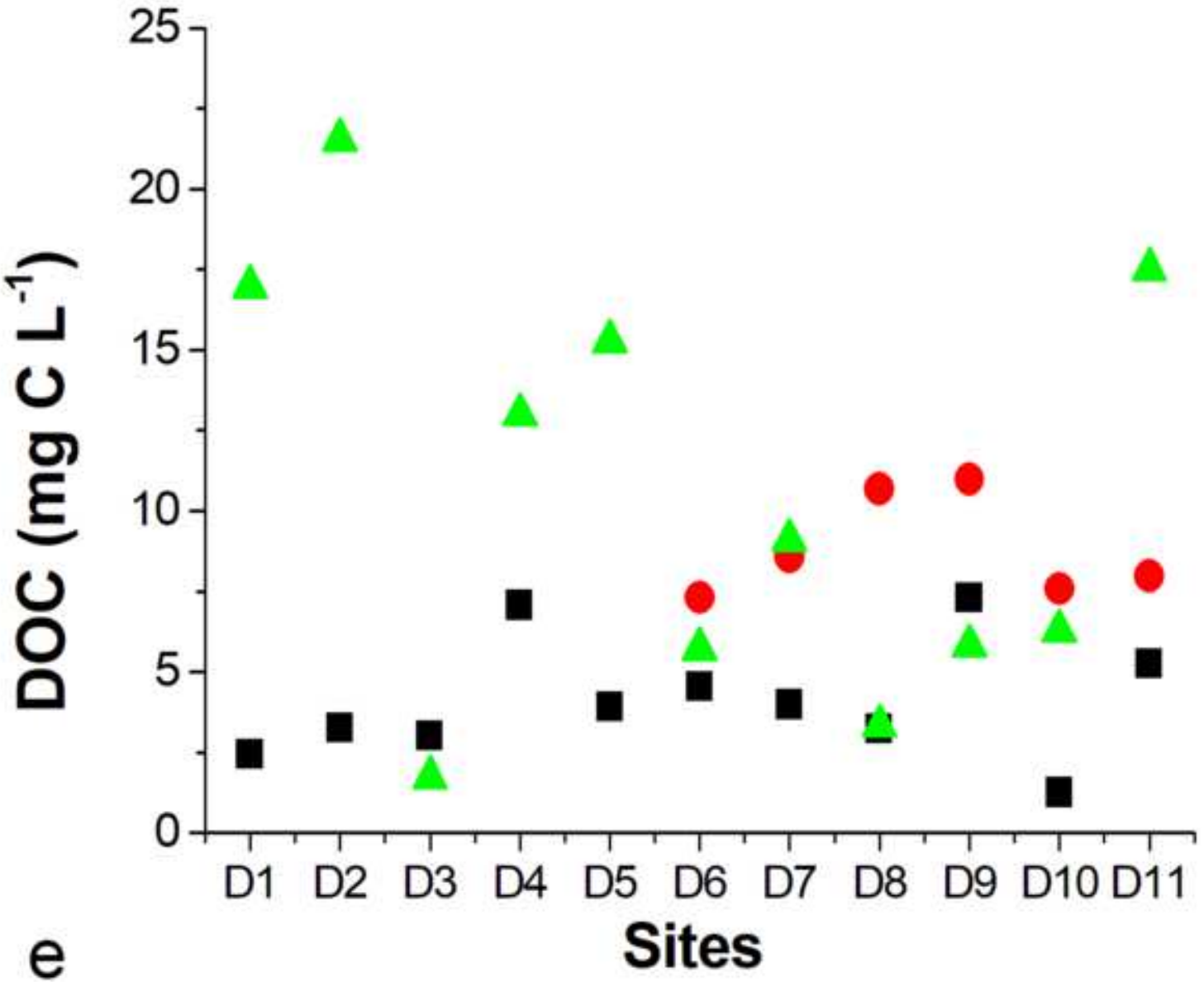

Figure 2f

Click here to access/download;Figure;Fig. 2f.BMP

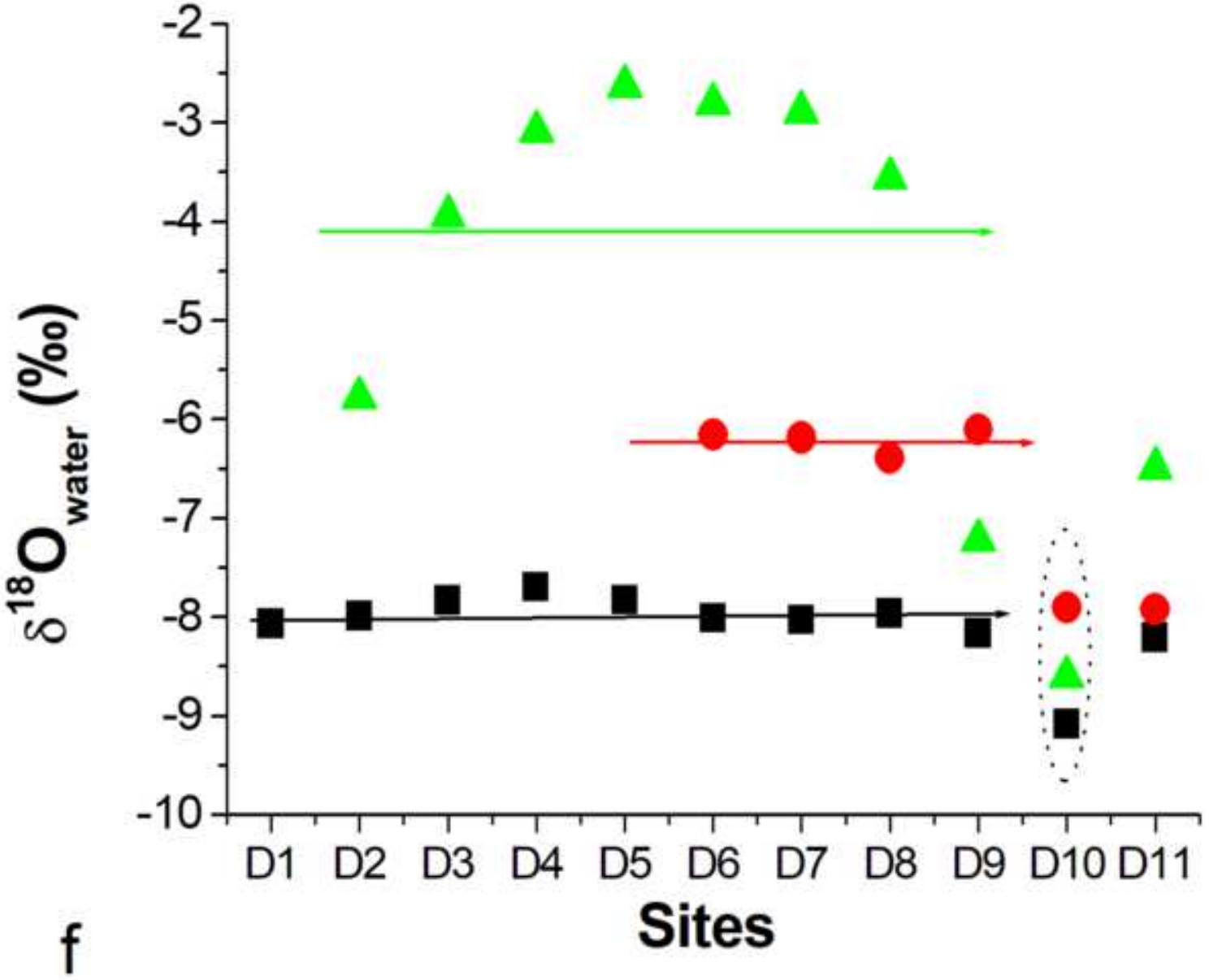

f

Figure 3a

Click here to access/download;Figure;Fig. 3a.BMP

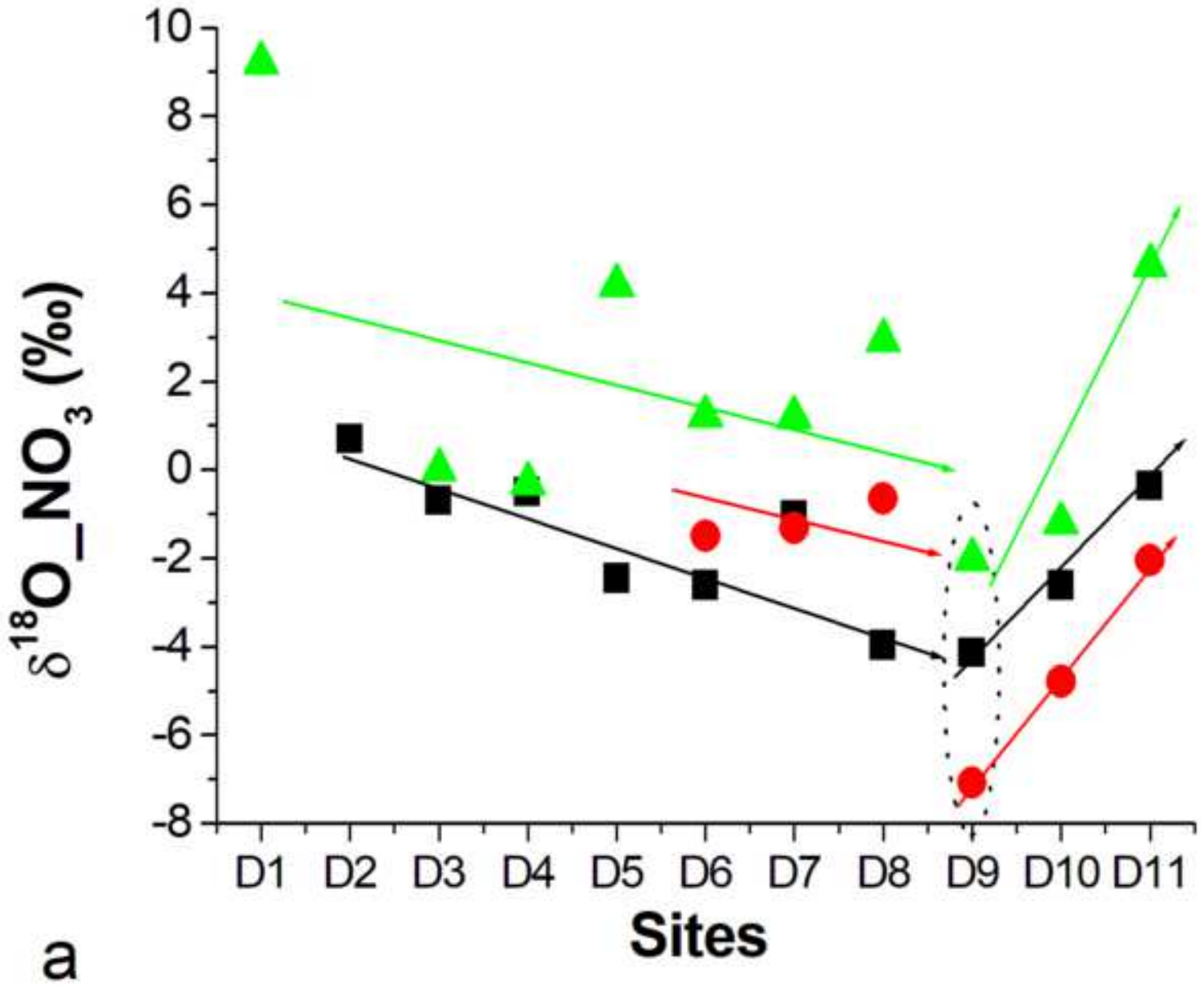

Figure 3b

Click here to access/download;Figure;Fig. 3b.BMP

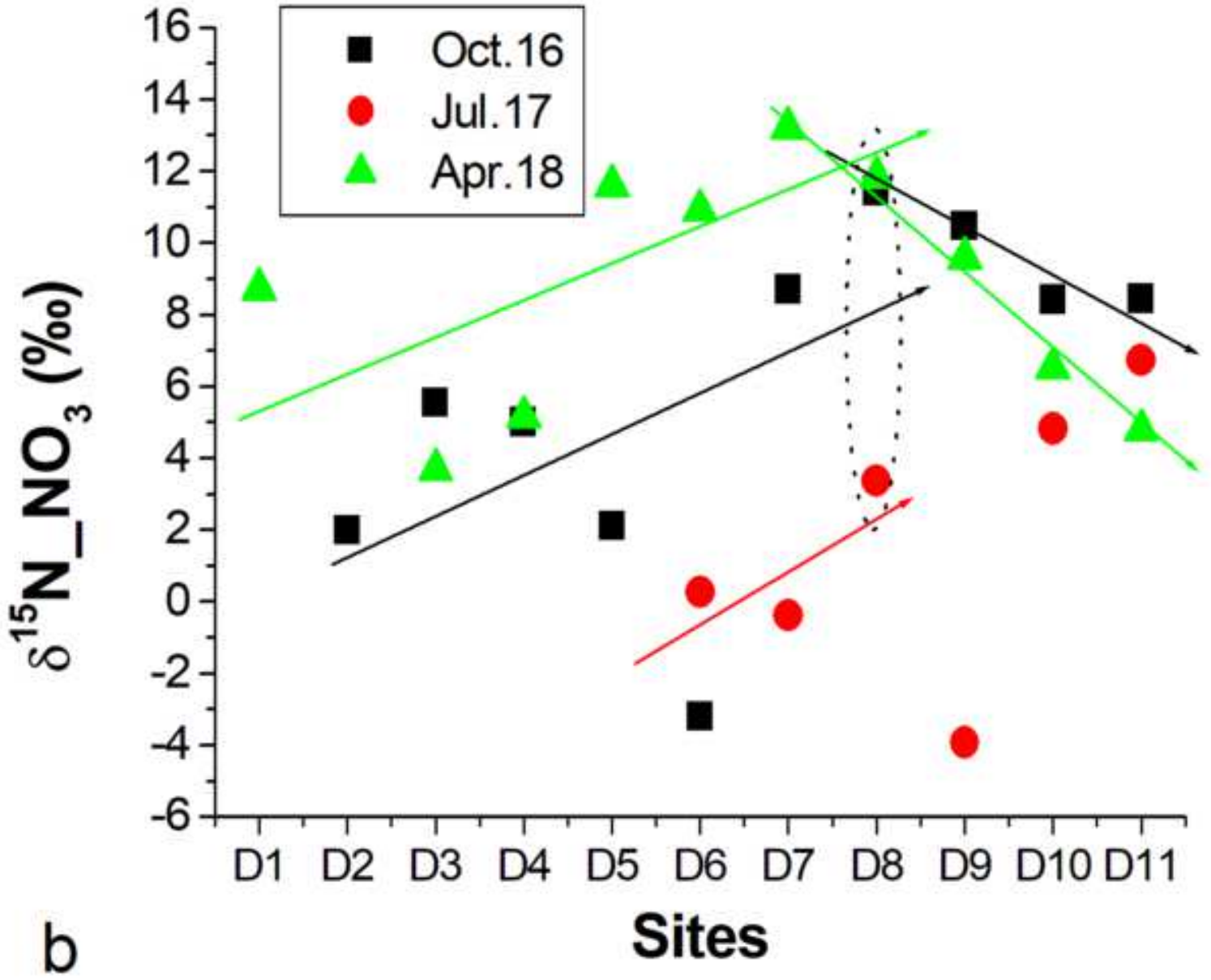

Figure 4

Click here to access/download;Figure;Fig. 4.BMP

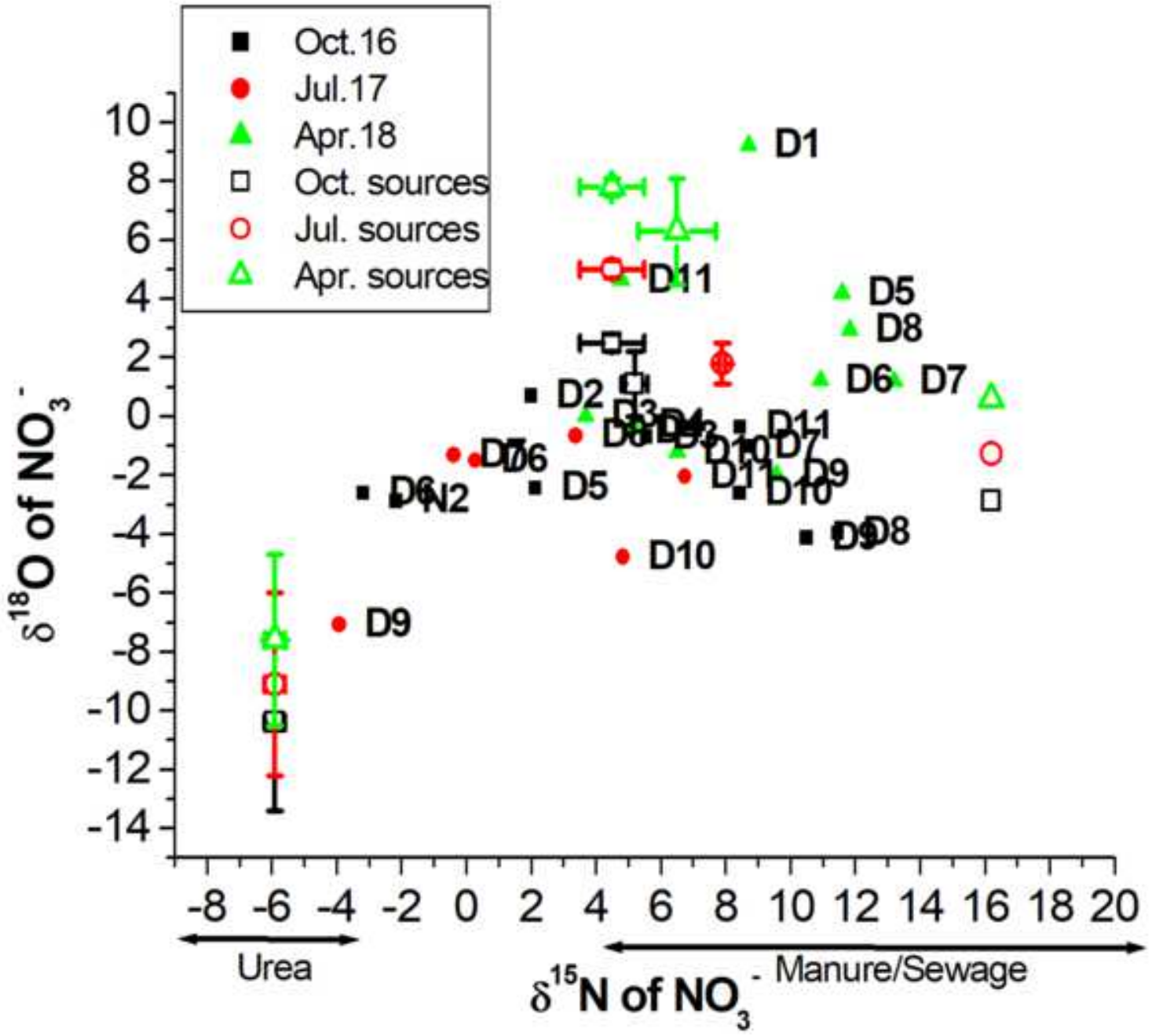

Figure 5a

Click here to access/download;Figure;Fig 5a PCA.bmp

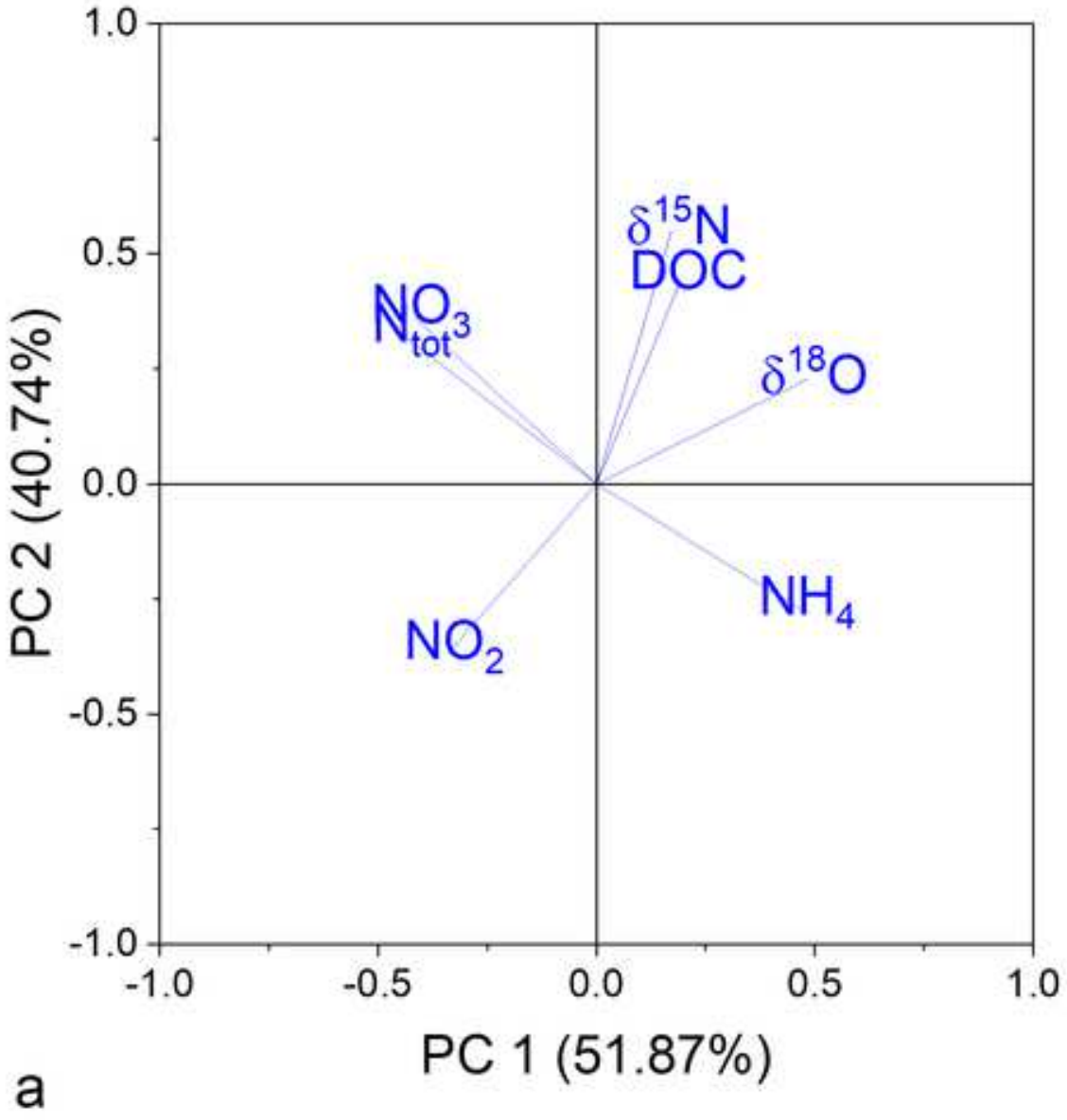

Figure 5b

Click here to access/download;Figure;Fig 5b PCA.bmp

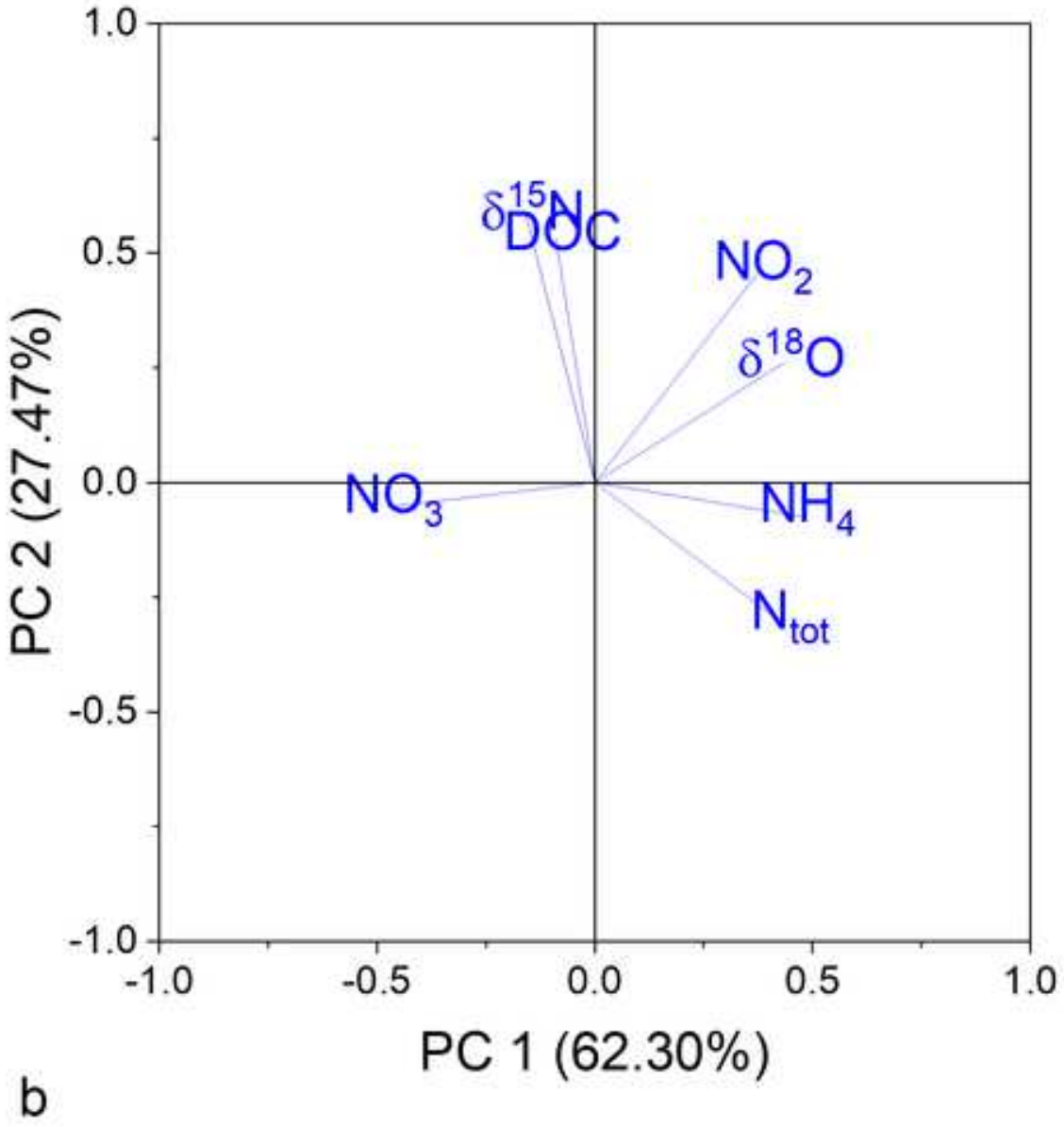

b